

**Load Testing, Model Calibration, and Analysis for a Three-Span
Reinforced Concrete T-Beam Bridge and a Highly Deteriorated
Filled Arch Bridge**

FINAL REPORT

**Prepared Under a Contract for Technical Support to
The U.S. DEPARTMENT OF TRANSPORTATION
FEDERAL HIGHWAY ADMINISTRATION NDE CENTER**

Submitted to

WEST VIRGINIA DEPARTMENT OF TRANSPORTATION

And

FEDERAL HIGHWAY ADMINISTRATION

Prepared By

Jeff Weidner, John B. Prader, Franklin L. Moon and A. Emin Aktan

Drexel University

April 21, 2009



Acknowledgements

The authors express their deep appreciation to their colleagues at the Federal highway Administration – Turner Fairbanks Highway Research Center for their confidence and support. We are especially grateful for the contributions made by Dr. Frank Jalinoos - Director of NDE Center, Dr. Hamid Ghasemi - Manager of Long-term Bridge Performance Program and Dr. Steven Chase, who recently retired as FHWA Chief Science Officer. Additionally, we would like to extend our gratitude to Tom Smith and Bert Buchanan at the WV FHWA Field Office.

West Virginia Department of Transportation has made major contributions to this research. From the outset, the writers had the opportunity to work closely with Frank Liss and John Taylor as well as several district engineers and their staff. This interaction was necessary because the challenges of the project demanded an effective government-academe partnership. The West Virginia DOT engineers who participated in this research were instrumental in the success of the research and we are indebted to them for their efforts.

Table of Contents

Acknowledgements.....	i
List of Figures.....	vii
List of Tables	ix
Executive Summary.....	xii
1 Introduction.....	1-1
1.1 Introduction to Research	1-1
1.2 Background – Smithers Bridge	1-1
1.2.1 Bridge Condition.....	1-4
1.3 Background – Michigan Avenue Bridge.....	1-6
1.3.1 Bridge Condition.....	1-7
1.4 Objectives and Scope	1-10
2 NDE Material Testing Program and Analytical Load Rating.....	2-11
2.1 Description of Material Testing Program.....	2-11
2.1.1 Smithers Material Testing.....	2-11
2.2 Material Testing Results.....	2-12
2.2.1 Concrete Sampling.....	2-12
2.2.2 Rebar Sampling.....	2-13
3 Preliminary Finite Element Modeling	3-15
3.1 Goals of Preliminary Modeling.....	3-15

3.2	Smithers Bridge Modeling	3-15
3.2.1	Geometric Modeling	3-15
3.2.2	3D Frame and Shell Model	3-16
3.2.3	3D Solid Model.....	3-16
3.2.4	Comparison of Preliminary Models.....	3-17
3.2.5	Modeling the Static Load Case	3-18
3.3	Michigan Avenue Modeling.....	3-18
3.3.1	Geometric Modeling	3-18
3.3.2	3D Solid Finite Element Model	3-19
4	AASHTO Load Rating Procedure	4-20
4.1	AASHTO LRFR Procedure	4-20
4.1.1	Single Lane Loading	4-20
4.1.2	Multi Lane Loading	4-20
4.2	Preliminary Load Ratings.....	4-23
4.2.1	Analytical Load Ratings	4-24
5	Experiment and Instrumentation Design – Static Test	5-25
5.1	Smithers Bridge Static Test.....	5-25
5.1.1	Instrumentation Plan - Smithers.....	5-25
5.2	Michigan Avenue Static Test	5-29
5.2.1	Sensor Selection.....	5-29

5.2.2	Vertical Displacement Gages.....	5-31
5.3	Data Acquisition.....	5-32
5.4	Installation Difficulties and Malfunctions.....	5-33
6	Static Load Test Results.....	6-35
6.1	Test Procedures	6-35
6.1.1	Smithers Bridge Load Test Summary.....	6-35
6.1.2	Michigan Avenue Bridge Load Test Summary	6-36
6.2	Load Test Results	6-36
6.2.1	Smithers Bridge Results.....	6-36
6.2.2	Michigan Avenue Results	6-45
6.3	Proof Level Load Rating	6-46
6.3.1	Smithers Bridge Load Rating.....	6-46
6.3.2	Michigan Avenue Bridge Load Rating.....	6-47
7	Experiment and Instrumentation Design – Dynamic Test.....	7-48
7.1	Excitation Methods	7-48
7.1.1	Instrumented Sledgehammer	7-48
7.1.2	Falling Weight Deflectometer (FWD)	7-48
7.1.3	Drop Hammer Machine	7-49
7.2	Instrumentation Selection.....	7-50
7.2.1	Sensor Selection.....	7-50

7.2.2	Data Acquisition	7-51
7.2.3	Layout and Reasoning – Smithers Bridge	7-52
7.2.4	Layout and Reasoning –Michigan Avenue Bridge.....	7-52
8	Dynamic Test Results	8-54
8.1	Dynamic Test Summary – Smithers Bridge.....	8-54
8.1.2	Drop Hammer Machine	8-55
8.1.3	Falling Weight Deflectometer.....	8-55
8.1.4	Dynamic Test Results	8-56
8.2	Dynamic Test Summary – Michigan Avenue Bridge	8-61
9	Post-Test Finite Element Correlation.....	9-62
9.1	General Calibration Procedure – Heuristic Method.....	9-62
9.2	Smithers Bridge Static Calibration.....	9-62
9.2.1	Updated Parameters	9-62
9.2.2	Comparison of Calibrated Model to Experiment.....	9-63
9.2.3	Calibration to Strain Data	9-67
9.2.4	Load Rating with Calibrated Model	9-67
9.3	Smithers Bridge Dynamic Calibration	9-68
10	Summary, Conclusions and Recommendations.....	10-70
10.1	Summary of Work Completed	10-70
10.2	Conclusions	10-71

10.2.1	Smithers Bridge	10-71
10.2.2	Michigan Avenue Bridge.....	10-72
10.2.3	Research Recommendations and Conclusions.....	10-72

List of Figures

Figure 1-1 - Smithers Bridge	1-2
Figure 1-2 - Location of Smithers Bridge (Southeast of Charleston).....	1-3
Figure 1-3 – Postings	1-3
Figure 1-4 - Plan and Section Developed Based on Field Studies	1-4
Figure 1-5 – Extensive Spalling on the Underside of the Pier Cap	1-5
Figure 1-6 - Spalling and Exposure of Beam Seat.....	1-5
Figure 1-7 – Typical Damage to Wearing Surface at the Piers and Abutments	1-6
Figure 1-8 – Seepage and Build-up at Pier Caps from Drainage Issues.....	1-6
Figure 1-9 - Michigan Avenue Bridge.....	1-7
Figure 1-10 - Voided Area on Michigan Avenue	1-8
Figure 1-11 - Missing Spandrel Wall and Void.....	1-9
Figure 1-12 - Longitudinal Crack in Web.....	1-9
Figure 2-1 – Approximate Core Layout.....	2-11
Figure 2-2 – Typical Bridge Core	2-12
Figure 2-3 - Machining of a Rebar Sample	2-13
Figure 3-1 - 3D AutoCAD Model with Creek and Service Road.....	3-15
Figure 3-2 - SAP2000 3D Frame and Shell Finite Element Model.....	3-16
Figure 3-3 - 3D ABAQUS Model.....	3-17
Figure 3-4 - Michigan Geometric Model.....	3-19
Figure 5-1 – Smithers Bridge Static Instrumentation Layout.....	5-26
Figure 5-2 - Rebar Strain Gage	5-27
Figure 5-3 - Stirrup Strain Gage	5-27

Figure 5-4 - Vertical Displacement Gage Mount	5-28
Figure 5-5 - Pier/Diaphragm Rotation Bracket.....	5-29
Figure 5-6 - Michigan Ave Static Instrumentation Layout.....	5-30
Figure 5-7 - Surface Strain Gage Mounting	5-31
Figure 5-8 - Temporary Signpost System.....	5-32
Figure 5-9 - Scaffolding Required to Reach the Middle Span.....	5-34
Figure 6-1 - Midline Displacements throughout the Test.....	6-37
Figure 6-2 - Line D Displacements.....	6-38
Figure 6-3 - Line C Strains	6-39
Figure 6-4 - Line D Strains	6-40
Figure 6-5 - Displacement Results - First Span w/ Load at Midline	6-41
Figure 6-6 – Midspan Displacement Comparison	6-42
Figure 6-7 - Strains in the First Span with Load at Midspan.....	6-43
Figure 6-8 - Comparison of Midline Strains between Spans.....	6-44
Figure 6-9 - Beam in Contact with the Ground	6-44
Figure 6-10 - Load versus Displacement of the Downstream Beam.....	6-45
Figure 6-11 - Load versus Displacement of the Downstream Beam.....	6-46
Figure 7-1 - Falling Weight Deflectometer	7-48
Figure 7-2 - Drop Hammer Machine	7-49
Figure 7-3 - Piezoelectric Accelerometer	7-51
Figure 7-4 - Capacitive Accelerometer.....	7-51
Figure 7-5 - Smithers Bridge Dynamic Instrumentation Layout	7-52
Figure 7-6 - Michigan Ave Bridge Dynamic Instrumentation Layout	7-53

Figure 8-1 - Impact on the Top Side of the Bridge.....	8-54
Figure 8-2 - Drop Hammer Test on the Bridge.....	8-55
Figure 8-3 - FWD Testing on the Bridge.....	8-56
Figure 8-4 (a) Real portion of the FRF derived from MIMO test on deck, (b) Imaginary portion of the FRF derived from MIMO test on deck	8-57
Figure 8-5: (a) Real portion of the FRF derived from MIMO test using the drop hammer, (b) Imaginary portion of the FRF derived from MIMO test using the drop hammer	8-59
Figure 8-6 - Mode Shapes from Sledgehammer Test	8-61
Figure 9-1 - Midspan Displacement Comparison - First Span	9-64
Figure 9-2 – $\frac{3}{4}$ Span Displacement Comparison – First Span.....	9-64
Figure 9-3 - 1/4 Span Displacement Comparison - First Span	9-65
Figure 9-4 - Midline Displacement of Second Span under Load	9-66
Figure 9-5 - Midline Displacement of Third Span under Load	9-66

List of Tables

Table 2-1 - Core Testing Summary- Smithers.....	2-12
Table 2-2 – Core Testing Summary - Michigan Avenue.....	2-13
Table 2-3 - Rebar Test Results - Smithers.....	2-14
Table 3-1 - Model Comparison.....	3-18
Table 4-1 - Load Ratings for HL-93 Design Truck	4-24

Table 6-1 - Proof Level Rating Factors - Smithers.....	6-46
Table 6-2 - Proof Level Rating Factors - Michigan Avenue	6-47
Table 9-1 - Model Statistics.....	9-63
Table 9-2- Load Ratings from Calibrated Model	9-67
Table 9-3 - Mode Shape Comparison	9-69
Table 10-1 - Load Rating Summary	10-71

Executive Summary

This report presents the results of both static and dynamic tests of two structures, the Smithers T-Beam Bridge and the Michigan Avenue Bridge located in Smithers, WV, including an intermediate investigation into a rapid bridge screening device. Conclusions for the rapid bridge screening investigation will be presented in a subsequent research status report.

Smithers T-Beam Bridge

The Smithers Bridge is located on Rt. 60 in Smithers, WV (Figure E- I). It is a three span, three lane, simply supported t-beam bridge with a skew. The bridge was posted at 37 tons for a two-axle truck. As Rt. 60 is a major thruway for truck traffic, the WVDOT was interested in raising the posting for this truck to the state legal load of 40 tons. This change would allow for removal of all posting signs. However, the bridge exhibits substantial deterioration, typically concentrated around the two central piers. There is spalling along the height of the pier, on the underside of the pier cap, and at the beam seat locations, with exposed and corroded rebar. The joints of the spans, directly atop the pier caps, show signs of drainage issues. At the span joint, the roadway surface is cracked, allowing water to enter the structure. Some water escapes to the top of the pier cap at the corners of the span. No specific drainage system is installed to protect these connections. The rest of the superstructure appeared to be in excellent condition and inspections indicated no signs of scour or other foundation related problems.



Figure E- I - Smithers Bridge

Due to the uncertainty caused by the damage and drainage issues, Drexel University Intelligent Infrastructure Institute was contracted to conduct a static load test. The bridge also served as an excellent opportunity to test the methodology and reliability of rapid bridge screening.

The NCHRP Manual for Bridge Rating Through Load Testing indicated that for this structure and the state legal truck of 40 tons, a proof load of 200 kips per lane, or 600 kips total was required. The bridge was loaded incrementally in the following order:

1. (3) Trucks Empty – 101 kips
2. (3) Trucks 1/3rd Full – 174 kips
3. (6) Trucks 1/3rd Full – 350 kips
4. (6) Trucks 2/3rd Full – 472 kips
5. (6) Trucks Full – 604 kips

After the proof load was reached, crawl speed and high speed tests were conducted using 2 or 3 trucks as well. In total, testing took one day to complete, with a minimal impact on the local traffic.

During the test, measurements were taken at numerous locations on the underside of the bridge. The first span was densely instrumented because of accessibility. The instrumentation on the other, less accessible spans was not as dense. The measured responses included vertical and lateral displacements, longitudinal strains, settlement of the beam seats and rotation of the diaphragm at the piers.

The proof load of 600 kips was reached without incident. The response of the bridge was generally linear, though a small amount of softening was seen at the higher load levels. This is indicative of cracking within the concrete and was expected. No large or unexpected nonlinearities were present. The maximum displacement seen was 0.134 in (3.4 mm) while the maximum strain was 167 microstrain.

Figure E- II shows the load versus displacement at midspan of each of the three spans when the load was at each respective point. The behavior is very similar between spans, remaining close to linear throughout the test. A similar plot of load versus strain can be seen in Figure E- III. In this case, the response at C3 appears to have deviated from the other midspan measurements. This was likely due to the proximity of the gage to a large crack in the diaphragm. The crack is shown in Figure E- IV. Based on the vertical displacements, it can also be said that the bridge showed very little continuity between spans. Almost no uplift was seen on the spans which were not directly loaded.

At the location of the damage to the beam seats (Figure E- V), vertical displacement gages were installed to monitor the relative vertical deformation of the beam to the pier. Any observed nonlinearity in these gages would indicate that damage was accumulating at that location. Figure E- VI shows the plot of load versus displacement at the beam

seats. The behavior remained linear throughout the test, indicating that the damage was likely caused due to some other mechanism besides loading. The magnitude of the response was very small as well.

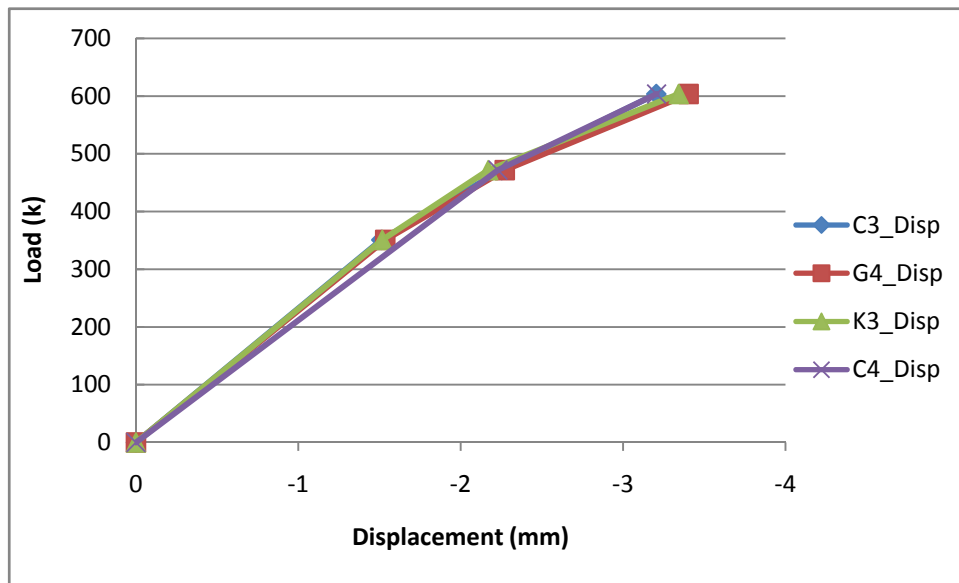


Figure E- II - Load vs. Displacement at Midspan of each Span

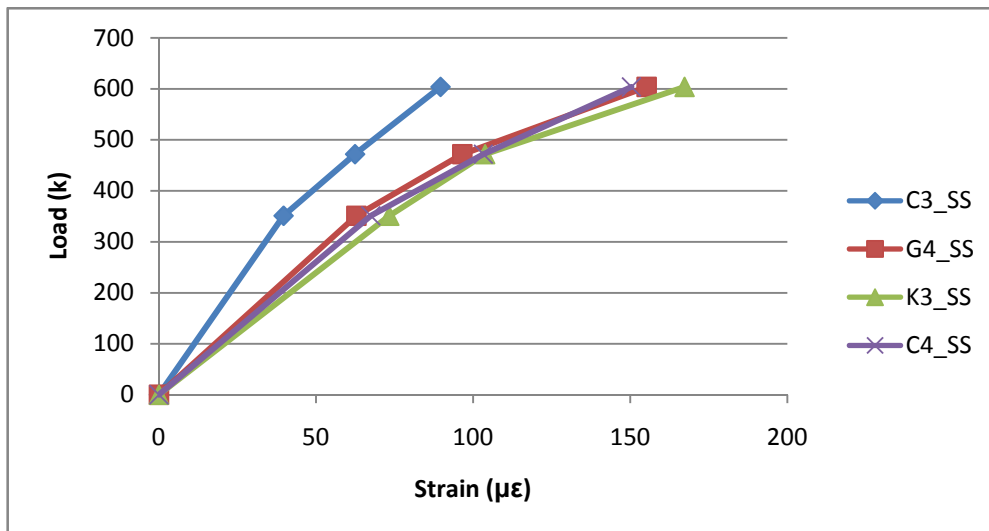


Figure E- III - Load vs. Strain at Midspan of each Span



Figure E- IV - Diaphragm Crack

Figure E- V - Damaged Beam Seat

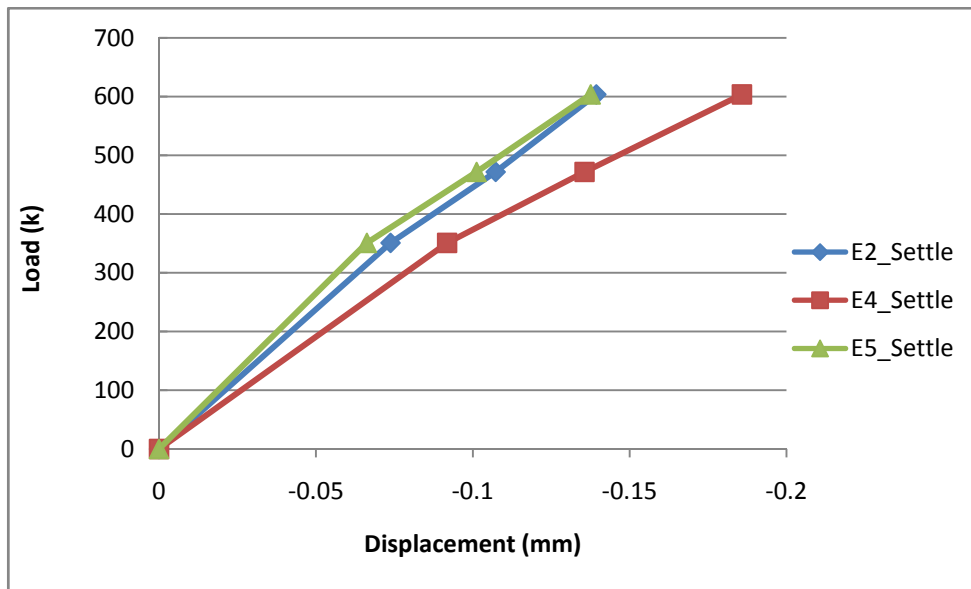


Figure E- VI - Minor Settlement of the Beams at the Damaged Beam Seat Locations

Table E- I shows the rating factors based on the state legal load of 80 kips using the NCHRP Manual for Bridge Condition Evaluation using Load Testing. The calculated proof load was 600 kips, which was reached during the final load case. Both rating factors are significantly greater than 1, indicating that with minor cosmetic repair, and adjustments to the drainage system, the posting can be removed.

Table E- I - Experimental Load Rating Factors

604 kip Load Stage		
Posting Level (Tons)	RF_O	RF_I
40	4.0	2.9

Where the spans meet at the pier caps, there is a full width diaphragm on each span. It appears that water is infiltrating between these diaphragms. When it rains, water can be seen escaping from the edges of the joint between the diaphragms, from underneath bearing plates for the beams, and from various cracks on the underside of the structure. This water infiltration should be mitigated through modification of the bridge's drainage system.

Michigan Avenue Bridge

The Michigan Avenue Bridge (Figure E- VII) was constructed in approximately 1900. Originally the structure was a single lane concrete arch bridge with a span of 34' and a height of approximately 7' above Smithers Creek. The bridge was widened using five reinforced concrete beams in the 1970's. This repair occurred before the responsibility of the bridge was turned over to the West Virginia Division of Highways (WVDOH) from the City of Smithers. The documentation and details of the original structure and the retrofit were not transferred to the WVDOH as they took ownership of this structure, and thus the only documentation currently available is inspection reports.

The arch portion of the bridge shows heavy deterioration on the spandrel walls, as seen in Figure E- VIII. Additionally, there are two long horizontal cracks at the base of either

side of the arch, which penetrate the width of the structure. On the upstream edge of the arch, a portion of the spandrel wall is missing, as well as the fill directly behind the exposed location Figure E- IX. The underside of the arch showed large voids, which were a result of using sizeable (in some cases larger than 6 in.) river stone as aggregate, see Figure E- X. Pachometer scanning revealed that no rebar was present in the arch.

The retrofit to the original arch bridge consisted of five reinforced concrete beams. Two of the beams lie on the upstream edge of the arch, and the other three are on the downstream edge. One of the downstream beams serves as a sidewalk and supports utility lines. It functions completely independent of the rest of the structure. The other four beams have very little connectivity between them; though there is some evidence of attempts to provide continuity between the upstream beams. The longitudinal cracks on the roadway surface at the edges of the arch are indicative of the lack of connectivity between the components. There are no details of the prestress forces or the rebar size and layouts for the beams. During the preparation for the test, concrete was chipped out along the underside of one beam in an effort to install steel strain gages and to explore the condition of the reinforcement. Though there are exposed stirrups visible on the sides of the beams, rebar could not be located from the underside without causing extensive damage. This investigation was stopped due to concern for the integrity of the beam. Currently the bridge is posted at 9 tons for a single axle truck. However, during the preparation for testing, some trucks and buses which appeared heavier than 9 tons were seen crossing the bridge.



Figure E- VII - Michigan Avenue Bridge



Figure E- VIII - Deterioration of Spandrel Walls



Figure E- IX - Void in the Arch and Prior Repair



Figure E- X - Large Visible Aggregate Pieces

The static instrumentation for the Michigan Avenue Bridge consisted of vertical displacements and longitudinal strains along the midline, and lateral displacement at either end of the arch. Since no rebar was found in the arch or the beams, the longitudinal strains were measured with a strain based displacement transducer mounted to the surface of the concrete. The vertical displacements were mounted to signposts cast into concrete blocks. No signposts could be driven into the ground due to the presence of a forced sewer main beneath the bridge. Displacements were the most reliable measurements taken, and were used in the decision making process. There were displacements measured on all four beams, as well as across the width of the arch.

The static test was conducted using two different loading sources at nine different locations. The bridge was loaded at $\frac{1}{4}$ span, midspan, and $\frac{3}{4}$ span along the centerline, in the upstream lane and the downstream lane. The load stages were as follows:

1. Work Van -7 kips (Figure E- XI)
2. Empty Single Axle Dump Truck– 17 kips
3. (2) Empty Single Axle Dump Trucks – 34 kips (Figure E- XII)
4. (2) Partially Loaded Single Axle Dump Trucks – 68 kips (Figure E- XIII)

The process used in the two truck load case was to back one truck into place, let the displacement reading stabilize and then back the second into place. The centerline was always loaded first, as the arch was the stiffest portion of the structure. Next the downstream lane was loaded, and finally the upstream lane. During these stages, two wheels of the truck were on the arch, and two wheels were directly on the inner of the two beams, as seen in Figure E- XIV.



Figure E- XI - First Load Stage (Work Van)



Figure E- XII - Third Load Stage (Two Empty Dump Trucks)



Figure E- XIII - Fourth Load Stage (Partially Loaded Dump Trucks)



Figure E- XIV - Left Side of Truck Loading the Beam Directly (Red Line is the Beam-Arch Interface)

The arch portion of the bridge behaved linearly until the 68 kip total load was reached using two partially loaded trucks. During the initial positioning of the first 34 kip truck on the downstream lane, large displacements and strains were observed. Rather than bringing on the other truck, it was decided that the load would be removed to check for linearity. When the load was removed, there was residual strain of $40\mu\epsilon$ and displacement of 0.01in, indicating that some plastic behavior had occurred. As a result of this nonlinearity, the test was stopped. Figure E- XV shows the load-displacement behavior of the arch, and Figure E- XVI shows the load-displacement behavior of the downstream

beam that displayed plastic deformation. The arch clearly remains linear while the beam displays nonlinear behavior (softening) after the 34 kip load stage under a single partially-loaded truck. It should be noted that when the two empty trucks were on the downstream lane, there was no nonlinear behavior observed, even though the load was approximately 34 kips total as well. This was likely due to the spacing of the wheels loads, which resulted in a smaller moment at mid-span.

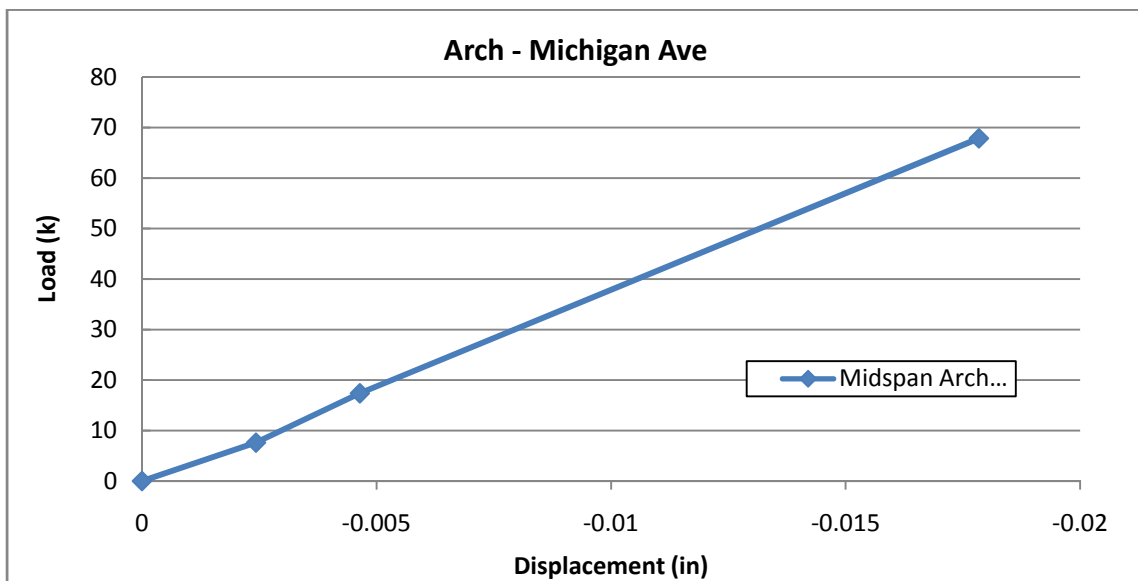


Figure E- XV - Load vs. Displacement - Arch

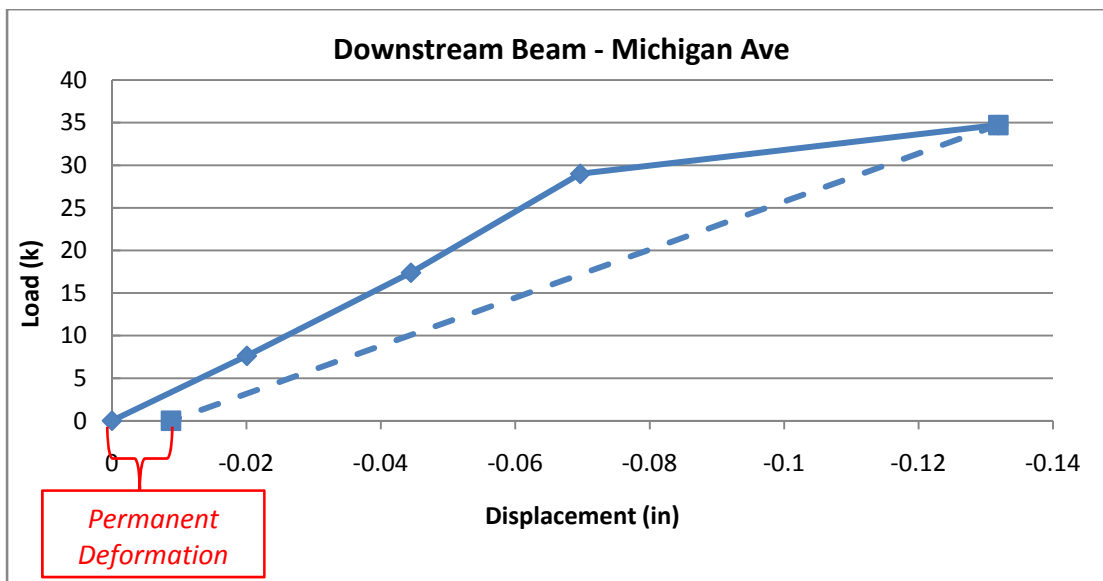


Figure E- XVI - Load vs. Displacement - Prestressed Beam

Post-test load ratings were calculated and are presented in Table E- II. The rating factors are based on the posted 9 ton truck using the NCHRP Manual for Bridge Condition Evaluation using Load Testing. The calculated proof load was 92 kips, which could not be reached. Neither of the resulting factors is above 1, indicating the posting should be lowered.

Table E- II - Experimental Rating Factors

31 kip Load Stage		
Posting Level (Tons)	RF_O	RF_I
9	0.94	0.69

Given the lack of reinforcement in this structure, the observed nonlinear deformation under 1/3 of the proof load level, and the extensive deterioration of both the reinforced concrete beams and the concrete arch, the replacement of this structure should be given

high priority. If immediate replacement is not feasible, we recommend that the Division of Highways take steps to remove truck traffic while limiting car traffic to the center, arch portion of the structure.

The dynamic testing of both structures consisted of a comprehensive multiple input – multiple output impact test using an instrumented sledgehammer. Impacts were record in sets of 5 at 38 different locations on Smithers Bridge and 15 locations on Michigan Avenue. Additionally, the modified Falling Weight Deflectometer, drop hammer machine, and an electromagnetic linear mass shaker were used to provide excitation on Smithers Bridge. The data from the additional excitation devices will be compared to the sledgehammer test to validate the effectiveness of rapid bridge screening for this type of structure. The results of the intermediate exploration into the FWD as a rapid bridge screening device will be presented in a subsequent research status report.

1 Introduction

1.1 Introduction to Research

The nation as a whole is facing a daunting infrastructure situation as a large portion of the assets that make up the infrastructure network have exceeded their expected life, and currently carry larger volumes and loads than those for which they were designed. Analytical load rating procedures depend heavily upon this information and are also generally geared towards simple, prismatic structural designs. As a result, these procedures are not applicable to undocumented structures or complex structures, such as filled arches. Given the uncertainty associated with such structures, their reliable rating requires an in-depth and integrated application of experimental and simulation technologies termed structural identification (St-Id). Such applications have the ability to clearly identify any sources of reserve capacity and redistribution mechanisms that, in many cases, result in the removal of postings, which were in place due to the uncertainty surrounding the capacity of the bridge.

1.2 Background – Smithers Bridge

The Smithers T-beam bridge (Figure 1-1) is a three span, simply supported concrete structure with a skew of approximately 18°. The bridge lies on Rt. 60 in Smithers, WV, about 30 minutes to the southeast of Charleston (Figure 1-2). Constructed in 1930, the Smithers Bridge spans Smithers Creek, and a service road. Each span is approximately 48' long; with a width along the skew is 48' as well. The bridge is currently posted 37T and 38T for a two and three axle truck respectively, as seen in Figure 1-3. Ideally, these trucks would be posted at the state legal load of 40T, allowing for removal of all posting signs. The posting for these two trucks was a result of the stress level at inventory, whereas the operating case was fine. This indicates that if there is

additional reserve capacity in the structure, the posting could potentially be removed. No drawings exist for this structure. Figure 1-4 shows the plan and section developed based on the field studies conducted by Drexel and WVDOH personnel.



Figure 1-1 - Smithers Bridge

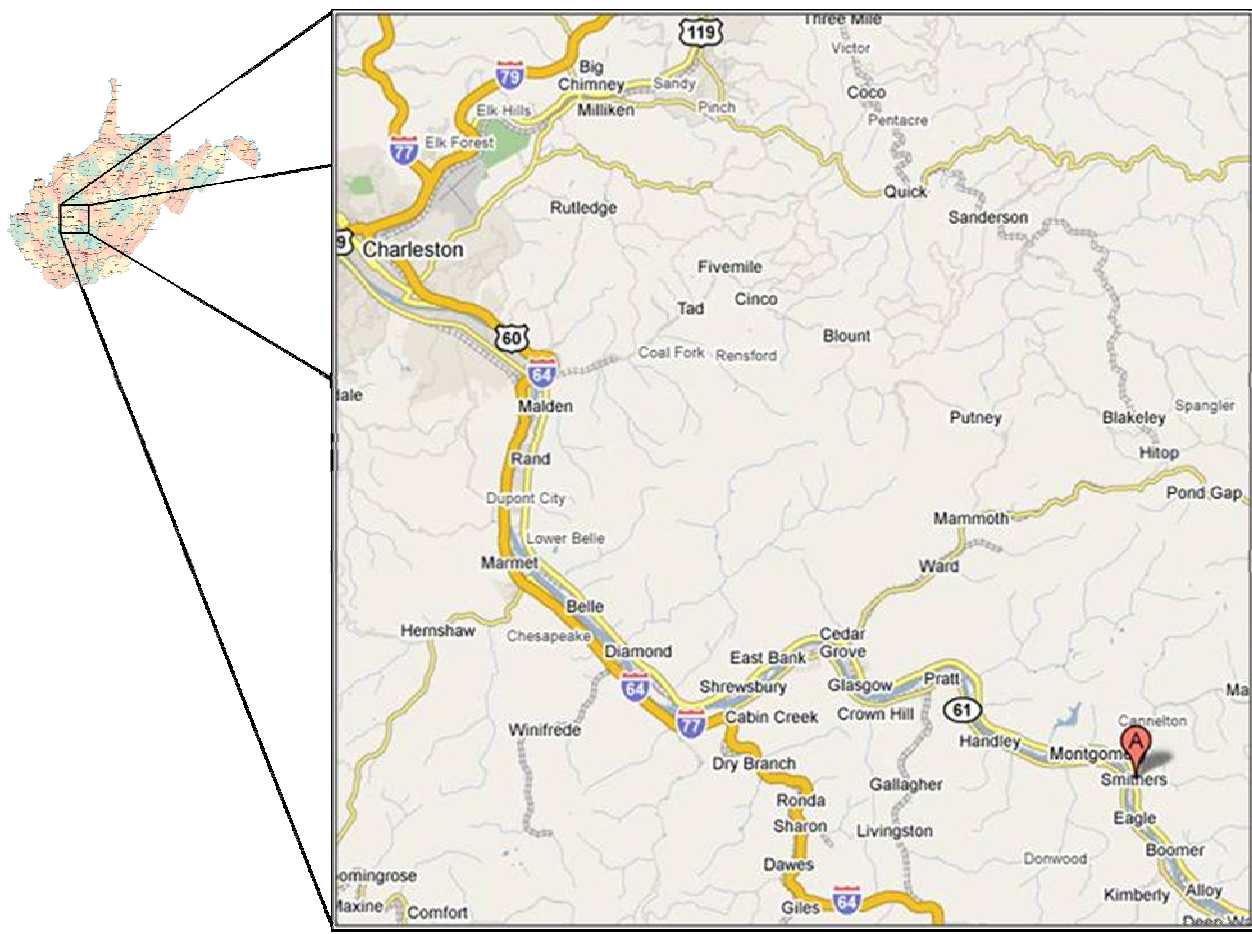


Figure 1-2 - Location of Smithers Bridge (Southeast of Charleston)



Figure 1-3 – Postings

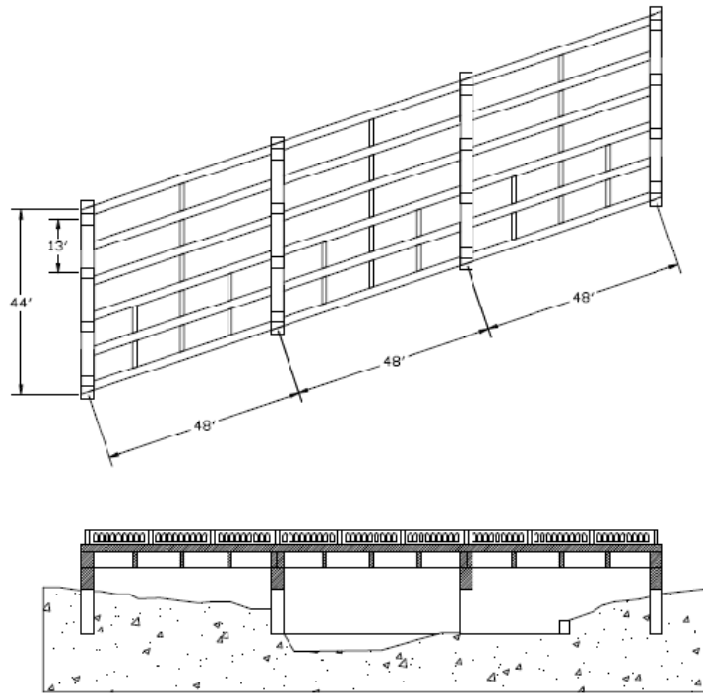


Figure 1-4 - Plan and Section Developed Based on Field Studies

1.2.1 Bridge Condition

The bridge exhibits some deterioration in critical locations. There is substantial spalling on the piers, pier caps and at some of the beam seats as seen in Figure 1-5 and Figure 1-6. The beams show flexural cracking, and some sparse locations of shear cracking. At the locations of the piers and abutments, the roadway surface shows substantial cracking (Figure 1-7). The bridge appears to have a serious drainage problem, with water seeping out from between the diaphragms and buildup of sediment atop the pier caps (Figure 1-8).



Figure 1-5 – Extensive Spalling on the Underside of the Pier Cap



Figure 1-6 - Spalling and Exposure of Beam Seat



Figure 1-7 – Typical Damage to Wearing Surface at the Piers and Abutments



Figure 1-8 – Seepage and Build-up at Pier Caps from Drainage Issues

1.3 Background – Michigan Avenue Bridge

During the site visit for the Smithers Bridge, WVDOH personnel pointed out a neighboring structure on Michigan Avenue (Figure 1-9) which also spans the Smithers Creek. The structure is comprised of an unreinforced concrete arch which was widened using five reinforced concrete

beams. The beams are an upside-down channel shape with two webs. It is not known whether the webs contain prestress or simple reinforcement. The bridge is 32' long and two lanes wide, with a sidewalk. The original structure dates back to the turn of the 19th century, while the addition came about around 1970. The bridge was originally managed by the city of Smithers, before being turned over to the WVDOH after the addition in the 70's. No original drawings of the arch or the addition exist. Due to the condition and age of the bridge, compounded by the lack of details, it is posted at 9 tons.



Figure 1-9 - Michigan Avenue Bridge

1.3.1 Bridge Condition

In general the condition of the Michigan Avenue Bridge is very poor. There are large horizontal cracks in the arch near the base, and patches of voided areas all along the underside (Figure 1-10). The spandrel walls are substantially deteriorated, and in one case, absent entirely, exposing a void beneath the roadway surface (Figure 1-11). The aggregate used for the arch appears to be river stone, and can vary in size up to approximately 6 inches. The beams, while

much newer, are in similar condition. There are long longitudinal cracks near the bottom of the webs which could be indicative of a bond failure (Figure 1-12). Between the components of the superstructure there is very little connectivity, resulting in extensive longitudinal cracks in the roadway. The eastern foundation is a scour hazard, already exhibiting substantial undercutting. The bridge is currently on the replacement list.



Figure 1-10 - Voided Area on Michigan Avenue



Figure 1-11 - Missing Spandrel Wall and Void



Figure 1-12 - Longitudinal Crack in Web

1.4 Objectives and Scope

The objective of this research was to rigorously investigate two structures of concern for the WVDOH. There was optimism that one of the structures could have a posting removed following a successful proof level test and structural identification. The other structure was a point of concern, already slated for replacement, which was tested mainly from an accessibility and efficiency stand point as the team was already working nearby. The scope of work includes:

1. Preliminary investigations into both structures including site visits, material property testing and development of documentation.
2. Development of 3D geometric models and finite element models for predictive and planning purposes.
3. Design of static and dynamic instrumentation to fully comprehend the behavior of both structures.
4. Carry out a proof level static load test and a suite of dynamic tests on each structure.
5. Model calibration and structural identification of the Smithers Bridge finite element model.
6. Develop recommendations and updated load ratings for both bridges.

2 NDE Material Testing Program and Analytical Load Rating

2.1 Description of Material Testing Program

2.1.1 Smithers Material Testing

The Smithers Bridge has a very uniform structure, and little variability was expected in the material properties that would result from the testing. As a result of this, an effort was made to limit the sampling to what was absolutely necessary. Three core samples were taken from each span of the bridge in a diagonal pattern, seen in Figure 2-1. Additionally, several samples were taken from the piers and abutments of the structure. A typical bridge core can be seen in Figure 2-2.

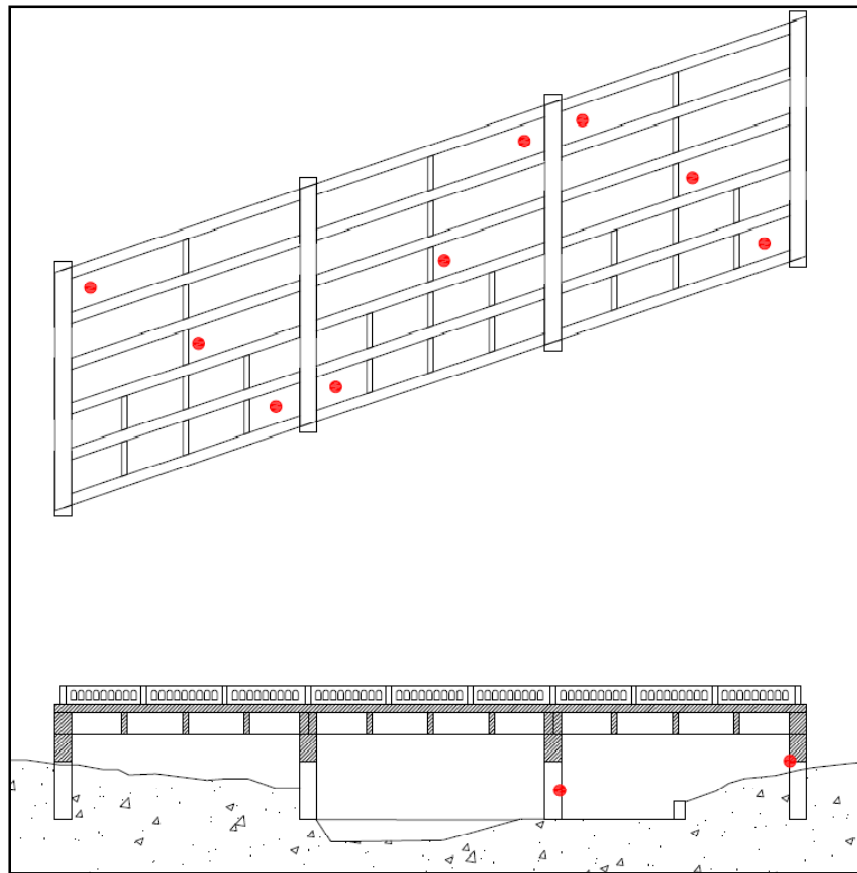


Figure 2-1 – Approximate Core Layout

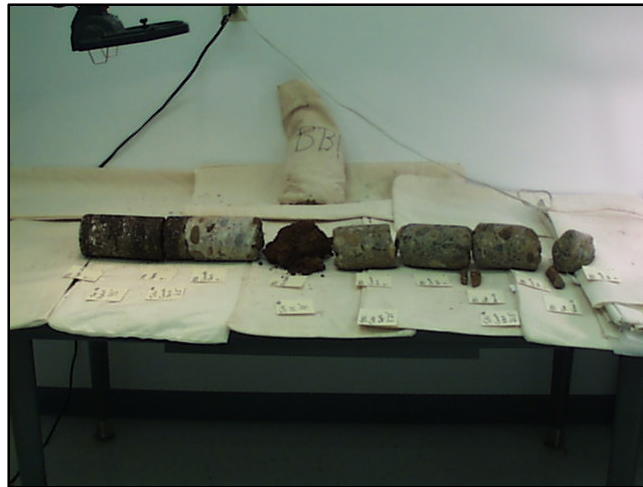


Figure 2-2 – Typical Bridge Core

2.2 Material Testing Results

2.2.1 Concrete Sampling

The samples taken from the Smithers Bridge were cut into ASTM standard sizes and tested in compression. The results are shown below in Table 2-1.

Table 2-1 - Core Testing Summary- Smithers

<i>Sample Designation</i>	<i>Concrete Compressive Strength (psi)</i>
S1	9302
S2	5969
S3	8361
S4	9468
S5	3950
S7	7424
S8	7204
SP1	7539
SP2	7551
SP3	9827
SP4	8556
<i>Average</i>	7741
<i>Standard Deviation</i>	1697

Due to the secondary nature of the Michigan Avenue test and the overall small scale of the bridge, only two samples were taken. The results can be seen in Table 2-2.

Table 2-2 – Core Testing Summary - Michigan Avenue

<i>Sample Designation</i>	<i>Concrete Compressive Strength (psi)</i>
SA1	4503
SA2	4829
<i>Average</i>	4666

2.2.2 Rebar Sampling

Rebar samples were taken from the bridge in addition to the concrete cores. The samples were machined down to ASTM standards for tensile specimens and then tested to determine yield and ultimate strength. A sample being machined can be seen in Figure 2-3. The results of the tensile tests for Smithers Bridge can be seen in Table 2-3. No samples were taken from Michigan Avenue.



Figure 2-3 - Machining of a Rebar Sample

Table 2-3 - Rebar Test Results - Smithers

<i>.505 Sample</i>	<i>Tensile Strength (psi)</i>	<i>Yield Strength (psi)</i>
<i>SR1</i>	72,177	47,500
<i>SR2</i>	78,132	48,900
<i>SR3</i>	82,900	37,500
<i>SR4</i>	98,289	64,500
<i>SR5</i>	89,090	60,000
<i>SR6</i>	73,166	27,758
<i>SR7</i>	75,286	49,500
<i>Average</i>	81,291	47,951
<i>Standard Deviation</i>	9552	12,513

3 Preliminary Finite Element Modeling

3.1 Goals of Preliminary Modeling

The goal of any a priori model is to roughly approximate the expected responses from a structure at given load stages, which serve as indicators during the test. Additionally, the instrumentation plan can be fine tuned to avoid pitfalls like installing gages in locations where the model indicates that responses will be minimal. The a priori model can be improved upon and calibrated post-test for a complete structural identification.

3.2 Smithers Bridge Modeling

3.2.1 Geometric Modeling

In order to fully understand the geometry of the Smithers Bridge, which had no documentation available, a 3-Dimensional model was created based on measurements taken during the preliminary field visit completed in August. The 3D model was created in AutoCAD and served as an excellent method for understanding the interaction of the components of the structure as well as a visual aid for instrumentation planning. The model is shown in Figure 3-1.

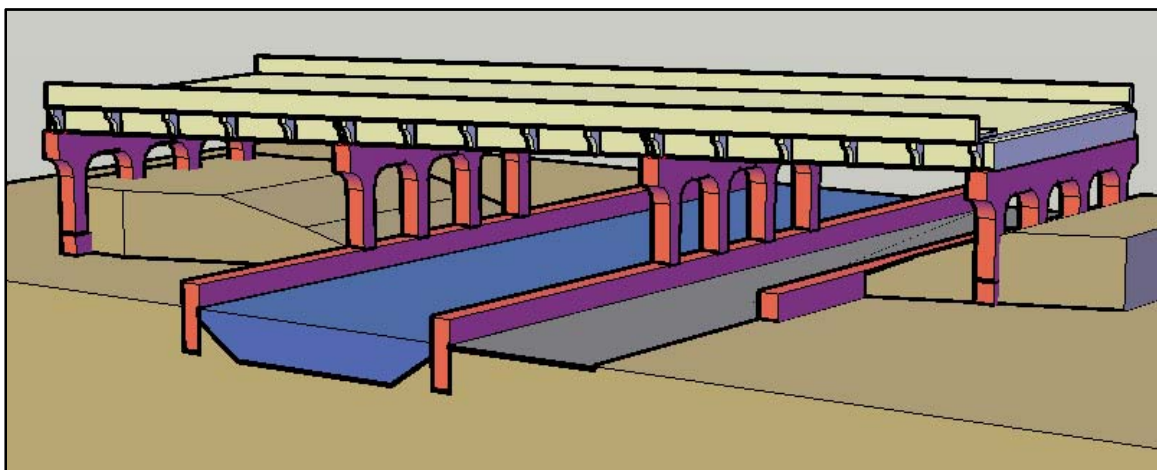


Figure 3-1 - 3D AutoCAD Model with Creek and Service Road

3.2.2 3D Frame and Shell Model

The Smithers Bridge is of simple construction, allowing for rapid, accurate finite element modeling. Unlike complex, multimaterial structures, like filled arches, the T-beam construction of Smithers Bridge is easily modeled using a combination of frame and shell elements. The preliminary model (Figure 3-2) uses frame elements to represent the beams, diaphragms and piers of the structure, and shell elements for the deck. The beams and the deck are connected using rigid links, forcing the components to act compositely. Likewise the beams are connected to the pier caps with rigid links. The support conditions at the abutments are pins, while the base of the piers is fixed. In total, the model is comprised of 1700 frame elements, 1900 rigid links and approximately 7000 shell elements.

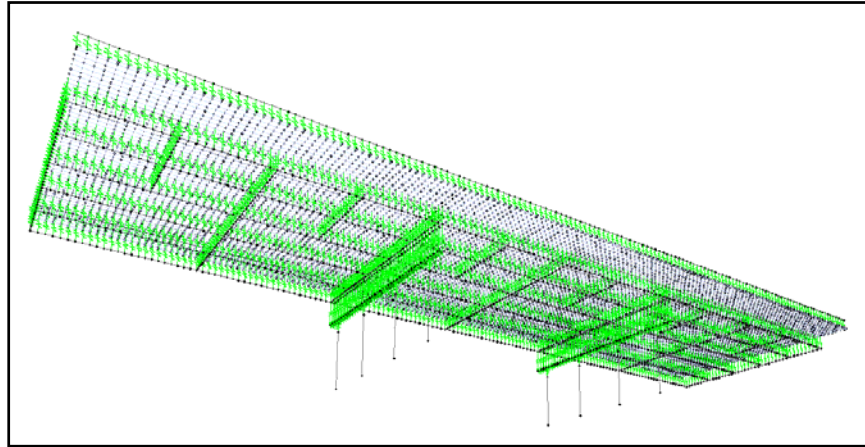


Figure 3-2 - SAP2000 3D Frame and Shell Finite Element Model

3.2.3 3D Solid Model

While the structure lent itself to a frame and shell element model using SAP2000, a 3D solid model using the ABAQUS software was created to serve as an independent check on the veracity

of the shell and frame model. The geometry created in AutoCAD was imported into ABAQUS to create the complete model. Quadratic tetrahedral elements were used for the beams, diaphragms and piers to allow for easier meshing as a result of the variable angles created by the skew. The deck, with simpler geometry was modeled using quadratic brick elements. The surfaces of the underside of the deck to the beams and diaphragms were constrained to each other rigidly using a tie constraint. This forces the components to act compositely by tying the nodes at the interface to each other. Figure 3-3 shows the complete model with contours representing the displacements due to dead load.

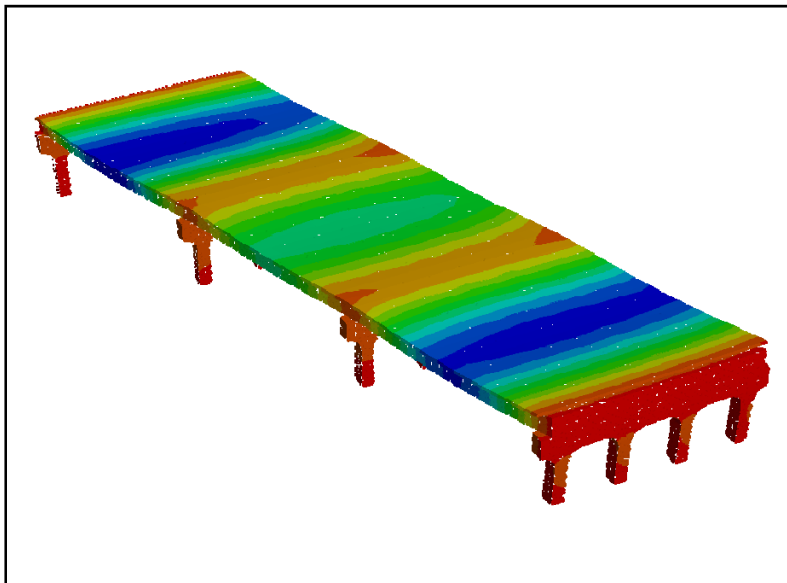


Figure 3-3 - 3D ABAQUS Model

3.2.4 Comparison of Preliminary Models

The models were compared at the midspan points of each span under the same loading scheme. The load consisted of a 100k point load at the middle on the first span. The displacement at the loading point is compared in Table 3-1. While the responses are on the same order of magnitude and are within 30% of each other, the solid model was stiffer. This can be attributed to continuity

at the piers which was left in place simply for convenience. The SAP2000 model had no continuity at the piers, representing the cracks in the roadway surface. These results indicate that the frame and shell element model is viable as an A priori model to be calibrated post-test.

Table 3-1 - Model Comparison

Model	3D Frame and Shell (SAP2000)	3D Solid (ABAQUS)
Midspan Deflection	-0.037 in	-.029 in

3.2.5 Modeling the Static Load Case

The model was loaded using estimated tire weights for six special dump trucks weighing approximately 100 kip each. The tire loads were represented as point loads on the surface of the shell element deck. The spacing of the truck tires was known from prior load tests, and the dense grid of shell elements allowed for very close approximation of the actual load distribution. The model predicted maximum displacements on the order of 0.125 in and strains of approximately 130 $\mu\epsilon$. These responses were reasonable and would serve as general guidelines for the test.

3.3 Michigan Avenue Modeling

3.3.1 Geometric Modeling

As with the larger structure, there are no drawings for the Michigan Avenue Bridge. Therefore, a 3D AutoCAD model was constructed based on the field measurements taken during the initial visit. The model consisted of the main components of the structure, the arch and the beams. Due to the uncertainty of parameters like connectivity and condition this model was used to create only one finite element model.

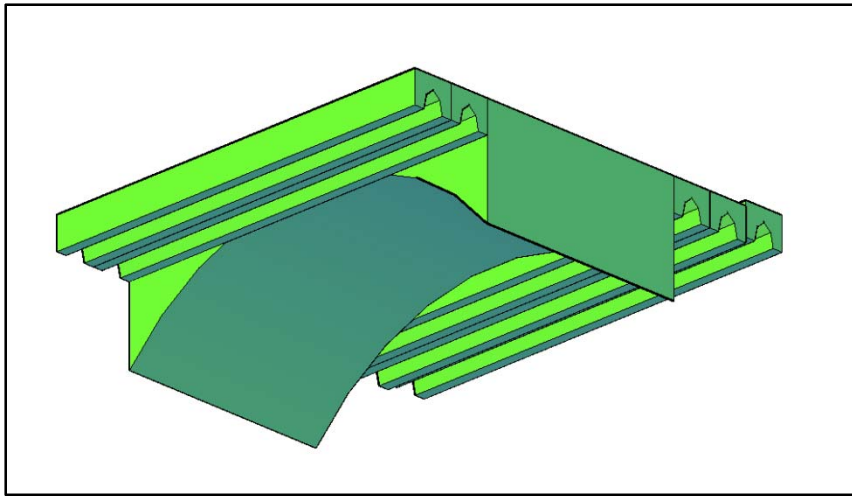


Figure 3-4 - Michigan Geometric Model

3.3.2 3D Solid Finite Element Model

The geometry created in AutoCAD was imported into ABAQUS and transferred into a solid 3D finite element model. This model was run under a few general load cases for the purpose of developing an understanding of the potential range of response which we could expect to see on the beams and the arch. Without an independent check, this information could not be utilized to provide test guidance, however several important conclusions were drawn as a result of this model. First, it became apparent that the interconnectivity between the beams and the arch was crucial, and that there were numerous potential limit states. Second, the model indicated that an arch of this span and dimension, if in excellent condition, would be very strong, and that quantifying the damage to the arch would be crucial for understanding its safety and reliability.

4 AASHTO Load Rating Procedure

4.1 AASHTO LRFR Procedure

The first step in rating a structure is to determine the geometry and material properties of the structure. If the material properties are unknown, AASHTO specifies recommended material properties in accordance with the structures' date of construction. The next step is to determine the width of the tributary area to which the dead load and live load will be distributed. This step and the associated equations apply to slab type structures. The AASHTO standard procedure to calculate the equivalent width tends to be conservative, particularly for analysis and rating of the existing bridges, which may cause unnecessary rerouting of the vehicles in certain circumstances (Amer et al., 1999). Therefore, FE analysis will also be used to analytically load rate the structures. The tributary width is determined as a factor of the length and width of the structure for slab type structures per equations 4-1 and 4-2:

4.1.1 Single Lane Loading

$$E_s = 10 + 5.0 * \sqrt{L_1 * W_1} \quad \text{4-1}$$

E_s is the tributary width that resists the loads applied for single lane loading. All longitudinal force effects are divided by this value to produce a per foot moment and shear. L_1 is taken as the lesser of 60 feet or the actual span length. W_1 is taken as the lesser of 30 feet or the bridges' true out-to-out width.

4.1.2 Multi Lane Loading

$$E_m = 84 + 1.44 * \sqrt{L_1 * W_1} \leq \frac{12 * W}{N_L} \quad 4-2$$

E_m is the tributary width that resists the loads applied for multi-lane loading. All longitudinal force effects are divided by this value to produce a per foot moment r shear. L_1 is taken as the lesser of 60 feet or the actual span length. W_1 is taken as the lesser of 30 feet or the actual bridge out to out width. N_L is the number of design lanes. W is the out-to-out bridge width.

The next step is to determine the dead load of the structure according to the physical geometry. The corresponding moment and shear caused by the dead load should also be calculated. The dead load moment and shear are distributed per foot by dividing the total dead load moment or shear by the tributary width for single or multi-lane loading. Single or multi lane loading is determined by the lane width of the structure. The third step is to determine the live load moment caused by the rating load applied to the bridge for single or multi lane loading. The maximum absolute live load moment should be used for rating purposes. The maximum shear due to the truckload should also be calculated in order to rate the structure for shear. The next step is to calculate the nominal moment resistance of the structure shown in equation 4.3. For the slab and arch structures the nominal moment resistance and nominal shear resistance is calculated per foot width of the structure. The nominal moment resistance is calculated based on the assumption of one way bending only. This assumption is very conservative and thus the rating factors will be conservative. The nominal moment resistance is calculated using equation 4-3.

$$M_n = (A_s * f_y) * \left(d_s - \frac{a}{2} \right) \quad 4-3$$

M_n is the nominal moment capacity of a one foot wide strip of the slab structure. A_s is defined as the cross sectional area of steel contained in a one foot wide strip of the structure. The term f_y is defined as the yield stress of the reinforcing steel. The term d_s is defined as the depth from the extreme edge of the compression fibers to the center of gravity of the reinforcing steel. The term a is defined as the depth of the compressive stress block. The next step is to calculate the nominal shear resistance of a one foot wide strip. The nominal shear resistance of each structure was calculated using equation 4-4.

$$V_c = 2 * \sqrt{f'_c} * b * d_v \quad 4-4$$

V_c is the nominal shear capacity of a one foot wide strip of the structure. The term f'_c is the compressive strength of the concrete. The term b is the width of the section and is taken as 12 inches. The term d_v is defined as the perpendicular distance between the resultant tension and compression forces and need not be taken less than $0.72*d$ as specified in AASHTO LRFD Article 5.8.2.7. The shear depth of the section is calculated using equation 4-5

$$d_v = d - \left(\frac{c}{2} \right) - 2 \quad 4-5$$

The final step is to calculate the rating factor for both shear and moment. Equation 4-6 is used in calculating the moment rating factor and equation 4-7 is used to calculate the shear rating factor.

$$RF = \frac{(\phi * \phi_c * \phi_s * Mn) - (\gamma_c * M_{DC}) - (\gamma_w * M_{DW})}{\gamma_{LL} * M_{LL}} \quad 4-6$$

$$RF = \frac{(\phi * \phi_c * \phi_s * Vc) - (\gamma_c * V_{DC}) - (\gamma_w * V_{DW})}{\gamma_{LL} * V_{LL}} \quad 4-7$$

RF is defined as either the inventory or operating rating factor depending on the modification factors chosen, i.e. γ_{DC} , γ_{DW} , and γ_{LL} . The dead load and live load moments and shears are modified by factors γ_{DC} , γ_{DW} , and γ_{LL} , which increase the effect of the dead load and live load on the structure. γ_{LL} is a magnification factor based on the average daily truck traffic crossing the structure. This factor is specified by AASHTO and located in Appendix A.6.2 Table 6-4 of the AASHTO LRFR manual. γ_{DC} , and γ_{DW} magnify the dead load moments due to the concrete and asphalt for the Strength I limit state. These values are given in AASHTO LRFR Appendix A.6.2 Table 6-3. The moment or shear capacity reduction coefficient is denoted by the Greek letter phi ϕ denotes the condition factor assigned to the bridge and is based on an engineer's best judgment of the condition of the structure. ϕ_s denotes the system factor for a structure and takes into account the superstructure type. These factors result in the AASHTO rating factors being a very conservative approximation of the real load rating of the structure. In the case of the Smithers Bridge, only the moment ratings will be presented.

4.2 Preliminary Load Ratings

4.2.1 Analytical Load Ratings

The Smithers Bridge was rated using the above procedure at both operating and inventory level. The ratings utilized updated material property information that was available after the material testing conducted by WVDOT. These ratings are shown in Table 4-1. It can be see that at operating level for the design truck, the Smithers Bridge is adequate. However, at inventory level, the rating was less than one. Note that due to the complex interactions of the components, the extent of damage, and the very low posting, pre-test load ratings were not conducted for the Michigan Avenue Bridge.

Table 4-1 - Load Ratings for HL-93 Design Truck

	RFO	RFI
Smithers	1.2	0.9

4.2.1.1 Load Rating Analysis

The load ratings calculated for the Smithers Bridge are consistent with the conclusions drawn based on the site visits to the bridge. Overall the bridge appeared to be in good condition, with the exception of the localized damage at the beam seats, under the pier caps, and at the junction of the spans. A rating at inventory of just below one is indicative of the age and condition of the bridge, but is far from condemning the bridge to removal from service. The innate conservatism in analytical ratings could easily be enough, if quantified, to raise the rating above one.

5 Experiment and Instrumentation Design – Static Test

5.1 Smithers Bridge Static Test

The Smithers Bridge was tested using proof load levels. The diagnostic test was skipped, though caution was exercised between load stages to verify that no damage was occurring. The load was applied using six special dump trucks capable of being loaded to total of 100 kips each. A dense array of instrumentation including several types of measurements was utilized to fully comprehend the response of the structure.

5.1.1 Instrumentation Plan - Smithers

5.1.1.1 Sensor Selection

The instrumentation of the Smithers Bridge included a total of 40 gages including rebar strains, vertical displacements, beam settlements, and rotations. The majority of the gages were focused on the easternmost span, as it was the most accessible from the underside. The other two spans were more difficult to reach and reference to, and therefore had minimal gages installed for the purposes of comparing the responses of the spans to the first. The gage layouts can be seen in Figure 5-1. Strain gages are represented by green rectangles, vertical displacements are red circles, lateral displacements are blue circles, rotation measurements are yellow triangles, and cyan circles are beam settlements.

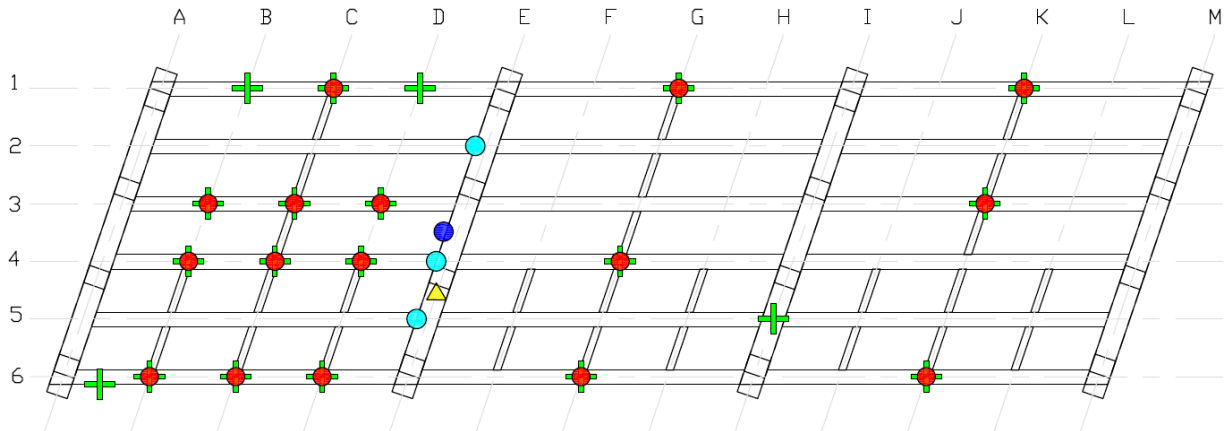


Figure 5-1 – Smithers Bridge Static Instrumentation Layout

5.1.1.2 Rebar Strain Gages

Based on the pachometer scanning conducted by WVDOT, 20 locations for weldable steel strain gages were chosen and the cover concrete was removed. These gages provide the most reliable and accurate measurements of steel strain. The weldable gages were obtained from Micro-Measurements Group. The gage model number is LEA- 06-W125E-350/3R (<http://www.vishay.com/strain-gages>). The gages come attached to a metal shim and are prewired, allowing for quick installation. Once the rebar is exposed and grinded smooth, the gage is microdot welded to the bar. Care is taken to be sure that the gage is aligned with the longitudinal direction of the rebar, so that the measured strain is as close to the actual axial strain as possible. The gage is then painted over to prevent any corrosion of the exposed steel. In addition to the longitudinal gages (Figure 5-2), several other gages were deployed for the purpose of measuring certain local responses, like strain in a stirrup at a shear crack (Figure 5-3).



Figure 5-2 - Rebar Strain Gage



Figure 5-3 - Stirrup Strain Gage

While these gages provide a reliable measurement of the actual steel strain, the fact that concrete has to be chipped away to expose the steel means that the measured response must be considered local.

5.1.1.3 Vertical Displacement Gages

For the purpose of measuring vertical displacements under the bridge, the more sensitive linear displacement transducers were preferred over linear potentiometers. The displacement gages were obtained from Texas Measurements Inc. (www.straingage.com) and manufactured by Tokyo Sokki Kenkyujo Co., Ltd (<http://www.tokyosokki.co.jp/e/index.html>). However, mounting the gages vertically is difficult. The sensor needs to be referenced to a fixed position, generally the ground. Due to the height of the structure, sign posts are driven into the ground, extended up to the underside of the bridge and braced out of plane. The gages are mounted to these posts and carefully aligned to ensure that they are measuring vertically (Figure 5-4).

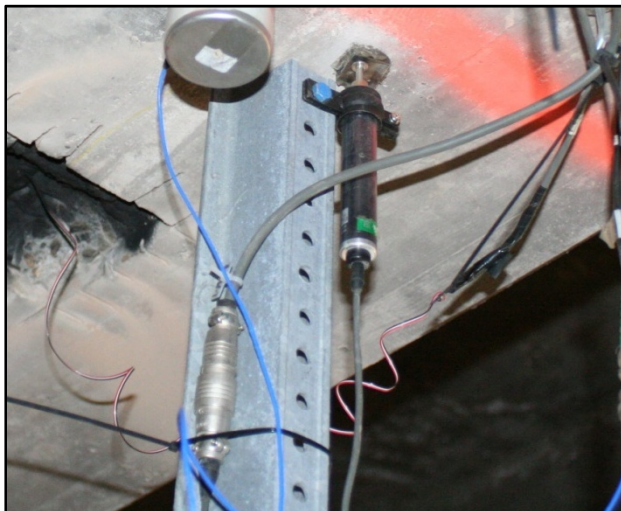


Figure 5-4 - Vertical Displacement Gage Mount

5.1.1.4 Rotation Gages

The rotation of the diaphragms above the pier caps in relation to the pier was of interest. A bracket was designed to mount to the pier and house the two displacement gages which, when combined could be used to determine the rotation of the diaphragms relative to the pier. The bracket is shown in Figure 5-5.

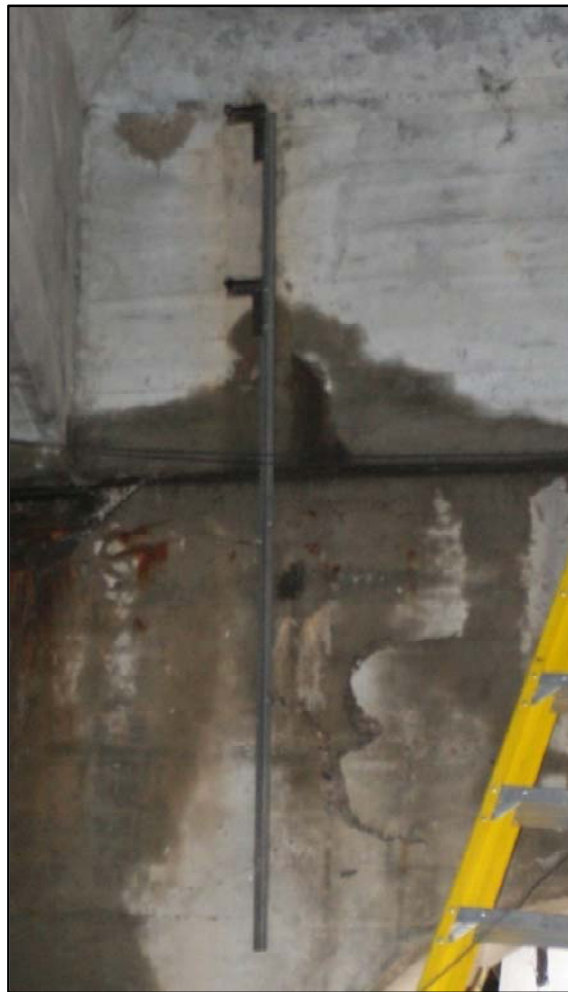


Figure 5-5 - Pier/Diaphragm Rotation Bracket

5.2 Michigan Avenue Static Test

5.2.1 Sensor Selection

The test of the Michigan Avenue Bridge used exclusively the strain based displacement transducers. This was because the pachometer scanning of the bridge indicated that no rebar was present in the arch, and the rebar in the concrete beams was too difficult to access. The sensor layout is shown in Figure 5-6 where a green rectangle represents a strain measurement, a red circle is a vertical displacement and a blue circle is a lateral displacement.

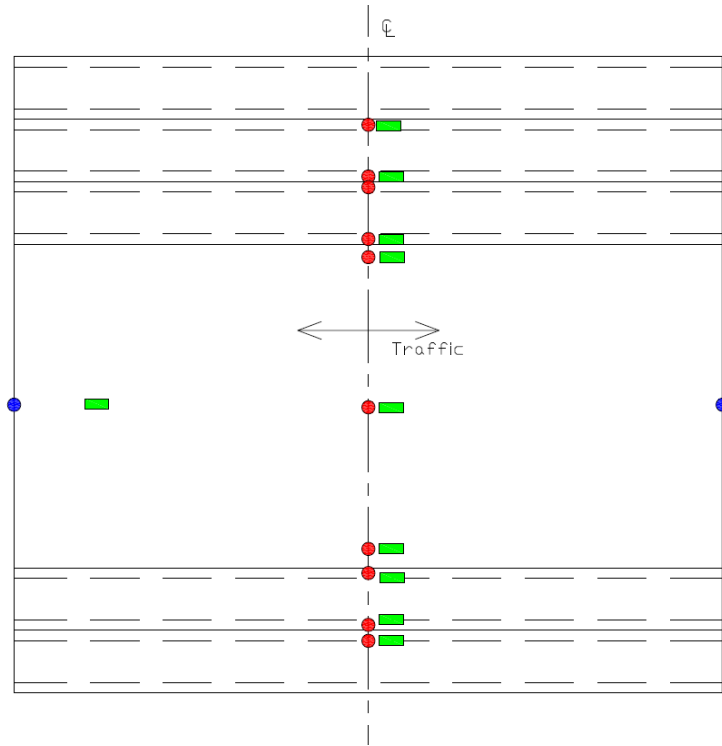


Figure 5-6 - Michigan Ave Static Instrumentation Layout

5.2.1.1 Concrete Strain Gages

Rather than a surface mounted strain gage, a linear displacement transducer was used to measure surface strains on the underside of the arch. It was mounted between two acrylic blocks, which were epoxied into holes on the underside of the arch or the beams. The gage was extended using rods in order to achieve the largest possible gage length. With the extension rods, the gage length was 12 inches. A mounted gage is shown in Figure 5-7.



Figure 5-7 - Surface Strain Gage Mounting

5.2.2 Vertical Displacement Gages

Due to the presence of utility lines under the Michigan Avenue Bridge, no signposts could be driven into the ground. The alternate method used was to cast signpost stubs into buckets full of concrete, and brace these posts out of plane to prevent any motion. The sign posts can be seen in Figure 5-8. A discussion of the performance of this system is included in Section 5.4.



Figure 5-8 - Temporary Signpost System

5.3 Data Acquisition

The Optim Electronics Megadac 3415 AC is a very rugged and reliable data acquisition unit. The Optim utilizes a chassis and removable card system for data acquisition. Two card types were utilized for these projects. Model AD305QB quarter bridge completion cards were used for the strain gages while model 808FB1 full bridge cards were used for all other gages. Each card accommodates 8 channels of data. The gages do not directly interface with the Megadac but rather with two types of STB modules which are shown in the Figure 11. The Optim uses a 16 bit Analog to Digital converter to convert the analog signal to a digital signal. The Optim can sample data as high as 25,000 samples per second. For the truck load test the data acquisition was set to sample at lower rates.

5.4 Installation Difficulties and Malfunctions

When compared to other structures, the access to the Smithers bridges was excellent. However, it was not without difficulties. The main problem was that the spans of both bridges which were over Smithers Creek were also spanning numerous utility lines buried in the creek bed. While the locations of these lines were known approximately, it was decided that sign posts would not be driven into the creek bed. Therefore some other method of displacement gage installation must be utilized. The final decision was to cast sign post stubs into a concrete block, and position the block at the proper location, building the support structure for the post extension off of that point (Figure 5-8). This allowed for gross adjustment of the gage by leveling out the bucket, and fine adjustment of the gage bracket attached to the post to achieve adequate alignment. This system was very effective for the Michigan Avenue Bridge but required substantially more bracing for the Smithers Bridge, which was taller. The middle span of the Smithers Bridge was so tall, that the buckets had to be placed on top of scaffolds placed in the river bed, as seen in Figure 5-9.

Despite the careful installation procedures and meticulous routing of cables, there were some gage problems which arose on test day. The most critical problem came from a bad displacement gage at location C4, the middle of the first span. The gage was removed and the sensor from location B6 was substituted in its place.



Figure 5-9 - Scaffolding Required to Reach the Middle Span

6 Static Load Test Results

6.1 Test Procedures

6.1.1 Smithers Bridge Load Test Summary

The static load test occurred Sunday November 16, 2008. Traffic control was available early in the morning, and the first trucks were brought on the bridge midmorning. Before the static cases were started, the trucks were run back and forth over the bridge with traffic to take some measure of the response under normal conditions. Next traffic was rerouted and the static load cases were started. The last static case was completed at 5pm and three crawl speed tests were done. The loading process for a given load level was as follows:

1. All six trucks were loaded at the offsite location approximately 8 miles from the bridge. Trucks were loaded with crusher run stone using a front end loader, and were weighed by WV Weight Enforcement personnel before departing to the bridge. Once three trucks were loaded they would depart and be used for preliminary load cases.
2. The other three trucks would come down to the bridge, and the first three would cross over the entire structure and park, facing away from the bridge. The other three trucks would turn around and back up to a similar position on the opposite side of the bridge.
3. Once all six engines were stopped, the Data Acquisition System would be balanced to zero prior to the loading of the bridge.
4. Each truck would back up one at a time to a position premarked on the bridge. After getting into position, the truck was shut off and data was recorded for at least 60 seconds, allowing the readings to stabilize. This process repeated for each truck until the entire load was reached.

5. The exact location of each truck was recorded using both pictures and video.
6. Once a sufficient amount of data had been recorded, the trucks were sent back for the next load stage.

6.1.2 Michigan Avenue Bridge Load Test Summary

The static load test occurred Saturday November 8, 2008. The bridge was shut down at 8am, and the morning consisted of dynamic testing. The first static case occurred at 1pm and the last static case was completed at 3pm. The load stages were as follows:

1. Loaded WVDOH work van – 7,000 lbs
2. Single empty dump truck – 17,000 lbs
3. Two empty dump trucks – 34,000 lbs
4. Single partially loaded dump truck – 35,000 lbs
5. Two partially loaded dump trucks – 69,000 lbs

6.2 Load Test Results

6.2.1 Smithers Bridge Results

6.2.1.1 Linearity Checks – Displacement

The bridge showed a generally linear response during the static load test. A slight softening indicative of some additional flexural cracking can be seen in some responses. The continuous diaphragm at Line C forces the structure to behave symmetrically at that line, which can be seen in Figure 6-1 as the responses at Line 1 and Line 6 are similar as well as those at Line 3 and Line 4.

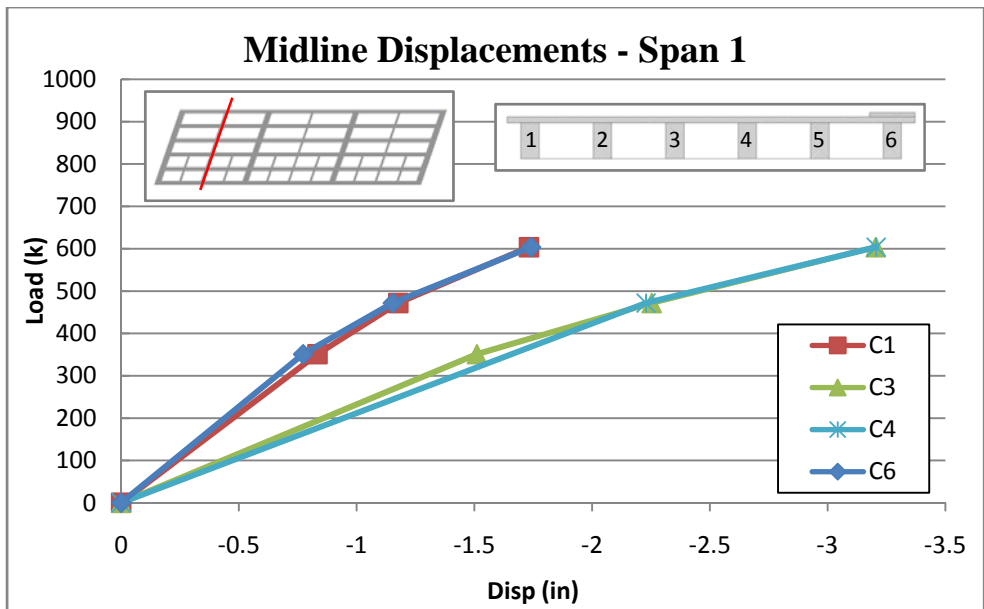


Figure 6-1 - Midline Displacements throughout the Test

At transverse locations where the diaphragm does not span the entire width of the bridge (i.e. Line B and Line D) the response is not as symmetric as the midline. In Figure 6-2, the displacements at Line D are shown. It can be seen that the displacement at D3 is substantially smaller than that of D4, which indicates that the load distribution without the diaphragms is not as widespread.

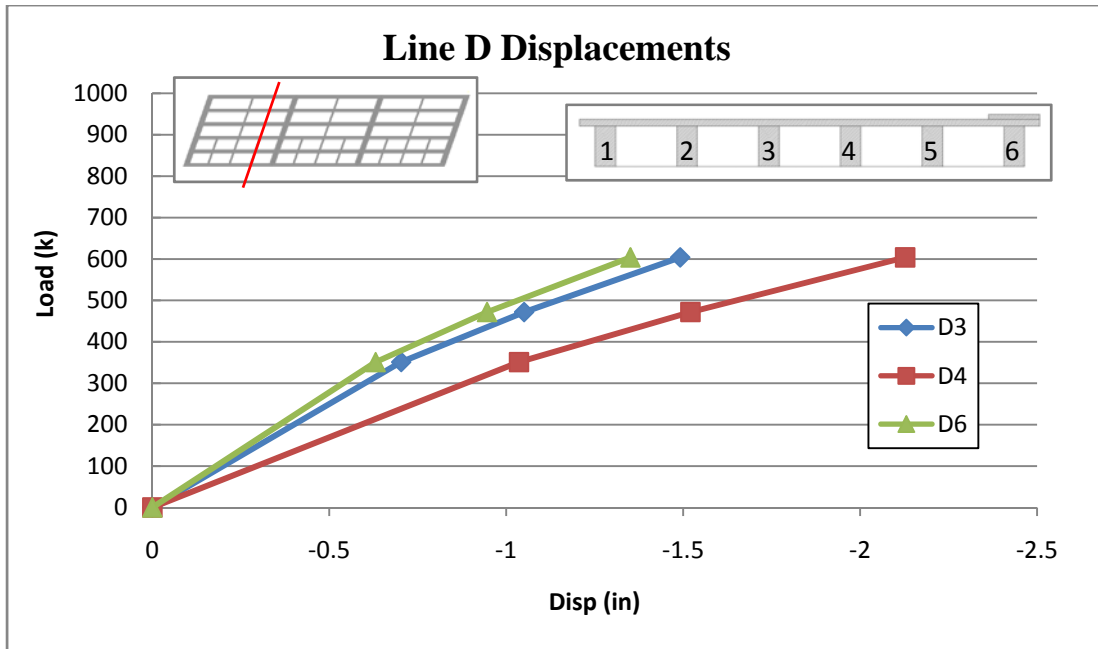


Figure 6-2 - Line D Displacements

6.2.1.2 Linearity Checks – Strain

Like the displacements, the strain values measured during the load test exhibit similar behavior; mainly that the response shows a slight softening throughout the test indicative of flexural cracking along the beams. Unlike the displacements, the strains are more susceptible to local effects. For this reason, the strain results presented here should be considered in the context that it is possible that the gage was placed directly adjacent to a crack in the concrete, thereby increasing the response dramatically. Any such local effects could not be predicted before the test and are unavoidable with local responses.

Figure 6-3 shows the longitudinal strain readings across Line C of the first span. In this case, the strain at C3 is likely decreased by the lack of load transfer across the diaphragm between line 3 and line 4, where a large crack was present.

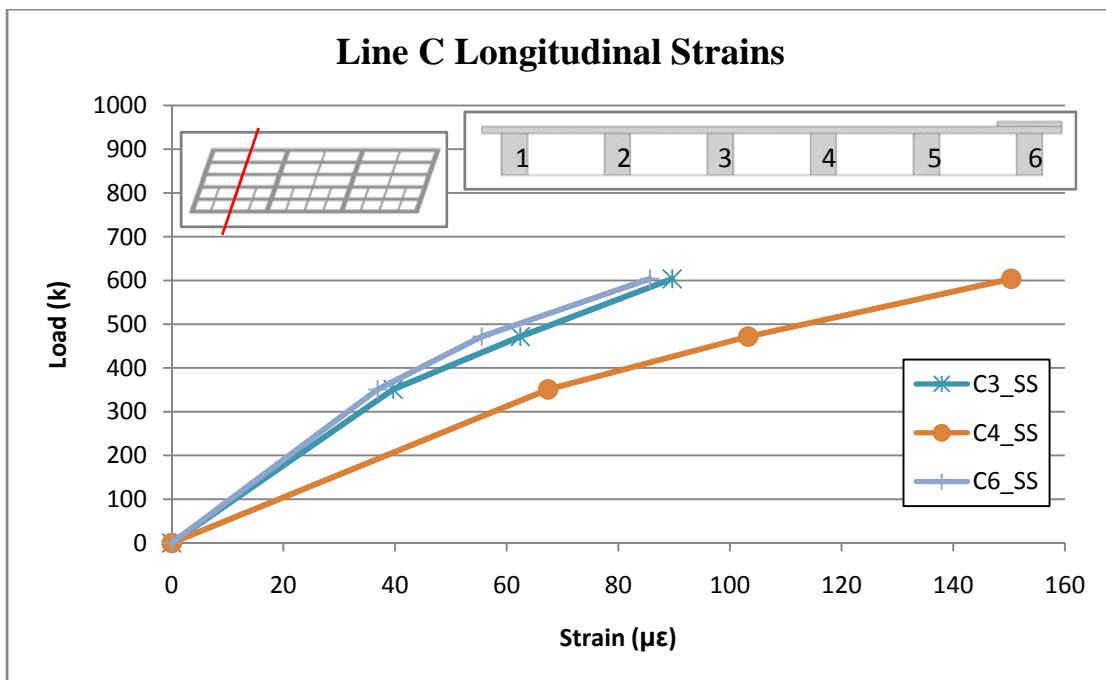


Figure 6-3 - Line C Strains

In the case of areas where the diaphragm did not extend, the differences in measured strains between beams can partly be attributed to varying load path caused by the lack of diaphragms. Figure 6-4 shows the strains along Line D where the diaphragm stops. The difference between strain at D6 and D1 as well as the difference between D4 and D3 can be attributed to the lack of a diaphragm to distribute load.

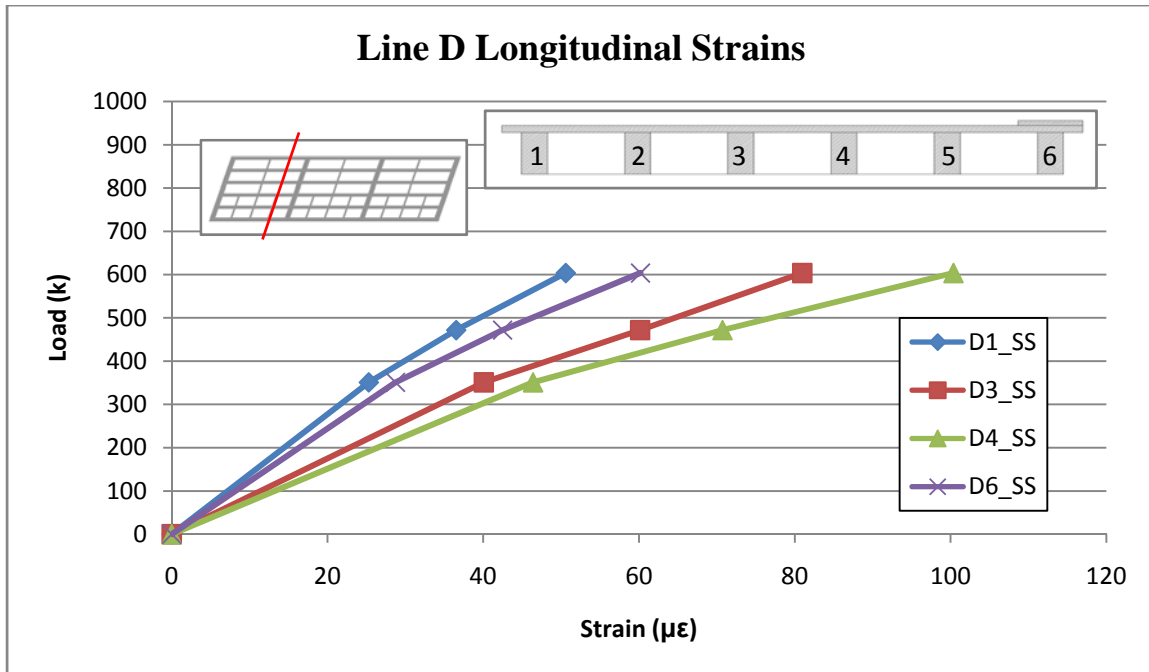


Figure 6-4 - Line D Strains

6.2.1.3 Final Load Stage - Displacements

Figure 6-5 shows the displacement profiles at $\frac{1}{4}$, $\frac{1}{2}$, and $\frac{3}{4}$ lines of the first span, with the load at midspan. As expected the largest response was at the midline, with proportionally smaller responses at $\frac{1}{4}$ and $\frac{3}{4}$ lines. As a result of the skew, the response at $\frac{1}{4}$ is slightly larger than at $\frac{3}{4}$ line.

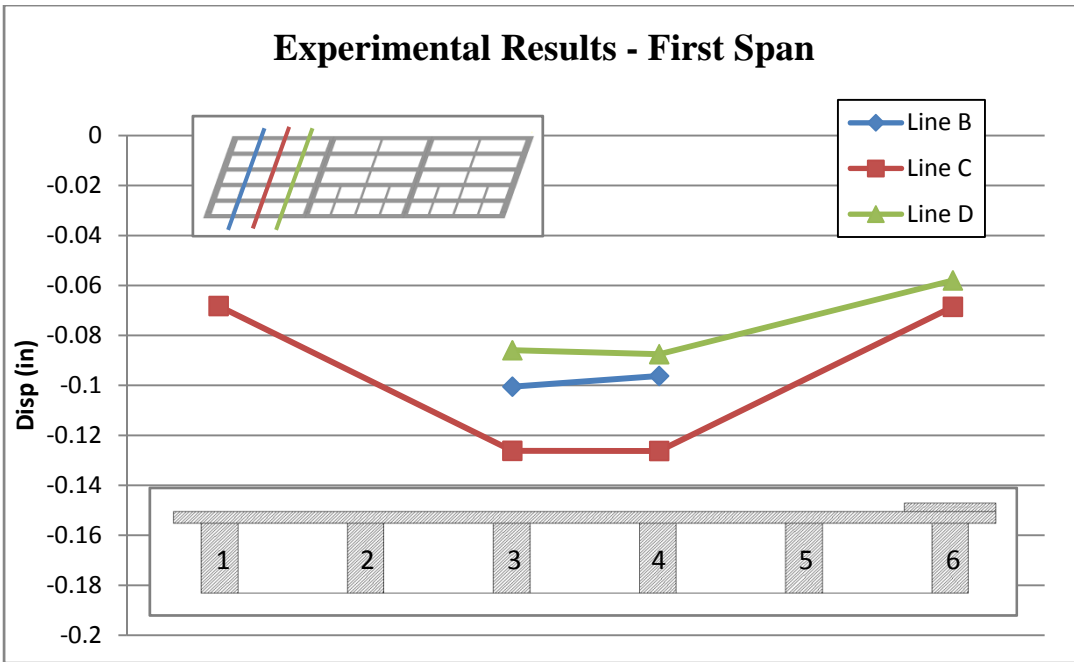


Figure 6-5 - Displacement Results - First Span w/ Load at Midline

Figure 6-6 shows a comparison between the displacements at midspan of all three spans versus each other. The purpose of this figure is to understand how similarly each span behaves to the first, heavily instrumented span. The first and third span seems nearly identical. The middle span has slightly different displacements at lines 1 and 4, which can be attributed to the varying boundary conditions provided by the more flexible piers, as opposed to the abutments.

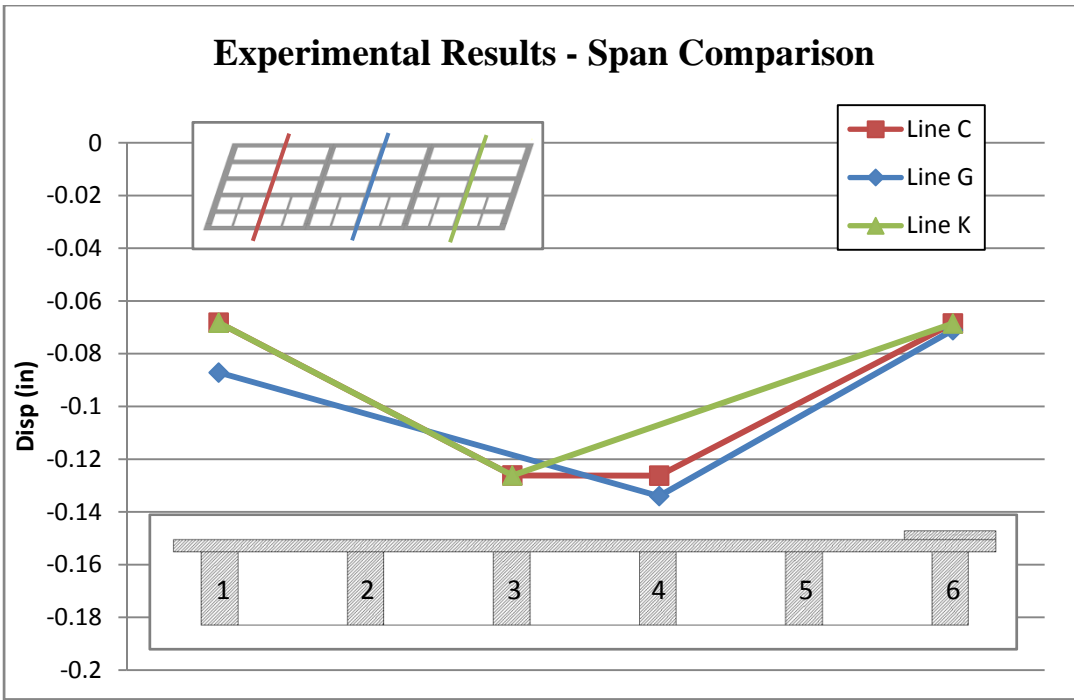


Figure 6-6 – Midspan Displacement Comparison

6.2.1.4 Final Load Stage – Strains

The strains measured on the first span with the load at midspan are shown in Figure 6-7. The response along Line 1 seems to increase with each successive transverse measurement. Unlike the displacements, the strain behavior seems to exhibit erratic behavior with no visible patterns. This is due to the local nature of the strain measurement. For example, directly adjacent to the location of the strain gage at C4, there was a large crack in the diaphragm which extended up to the deck. This proximity of this crack is likely responsible for the spike in strain at location C4.

Experimental Results - First Span

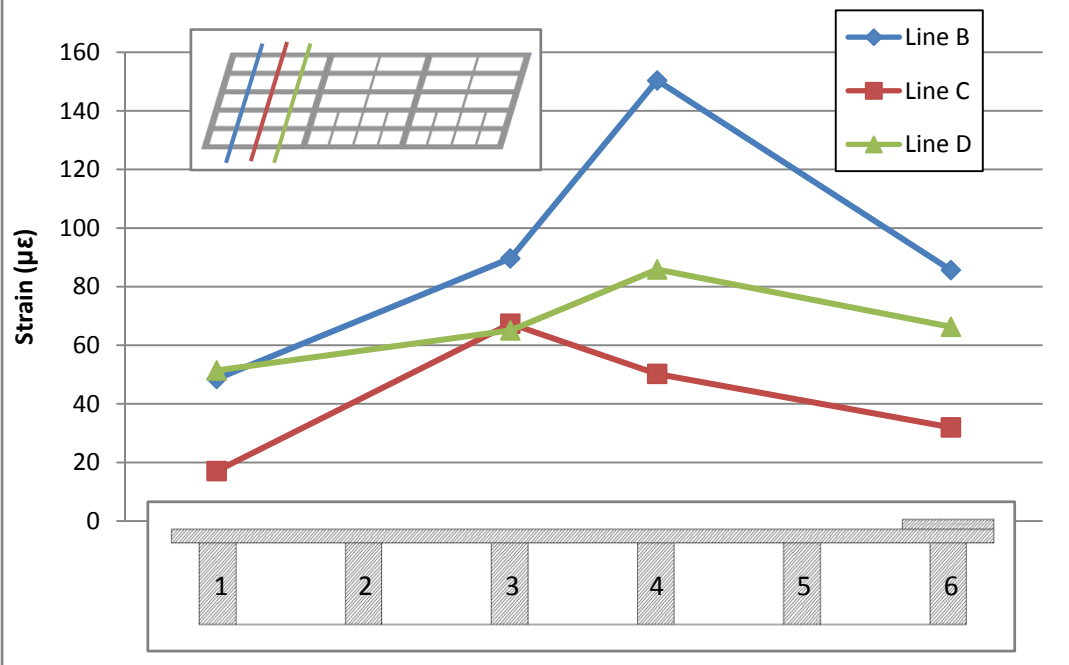


Figure 6-7 - Strains in the First Span with Load at Midspan

Figure 6-8 shows the strains along the midline of all three spans. While the displacements indicated excellent correlation between all three spans, the strains seem to indicate that a large portion of the load that transferred to Line 1 on the second and third span was not present in the first span. This could be attributed to several causes including the crack in the diaphragm or the partial supporting of the beam at Line 1 of the first span, shown in Figure 6-9.

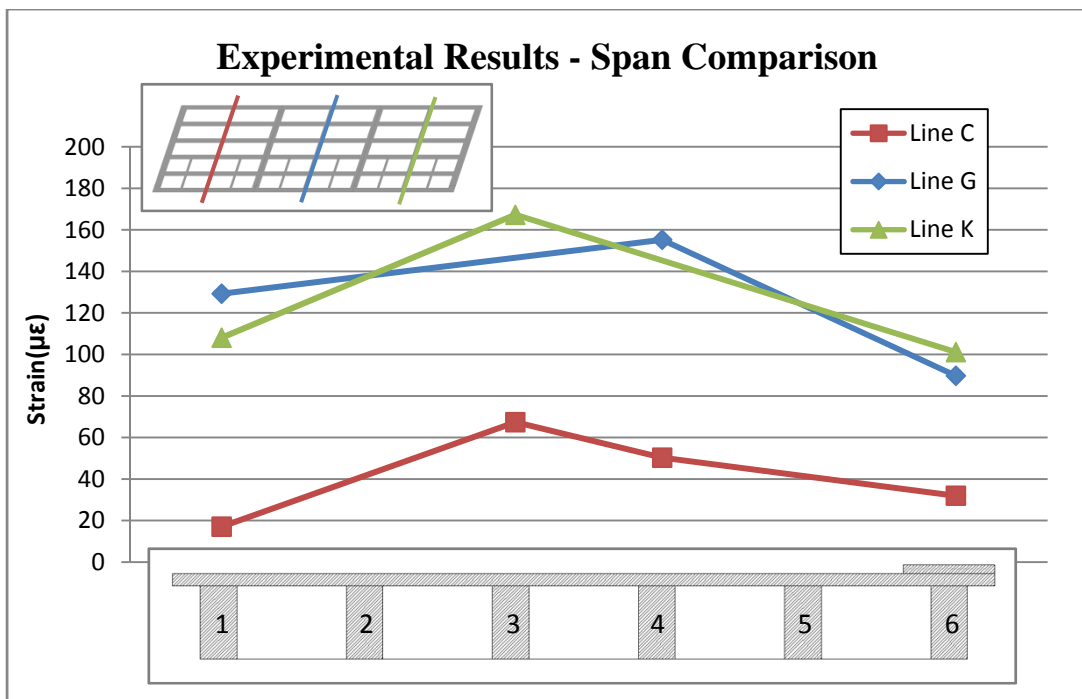


Figure 6-8 - Comparison of Midline Strains between Spans

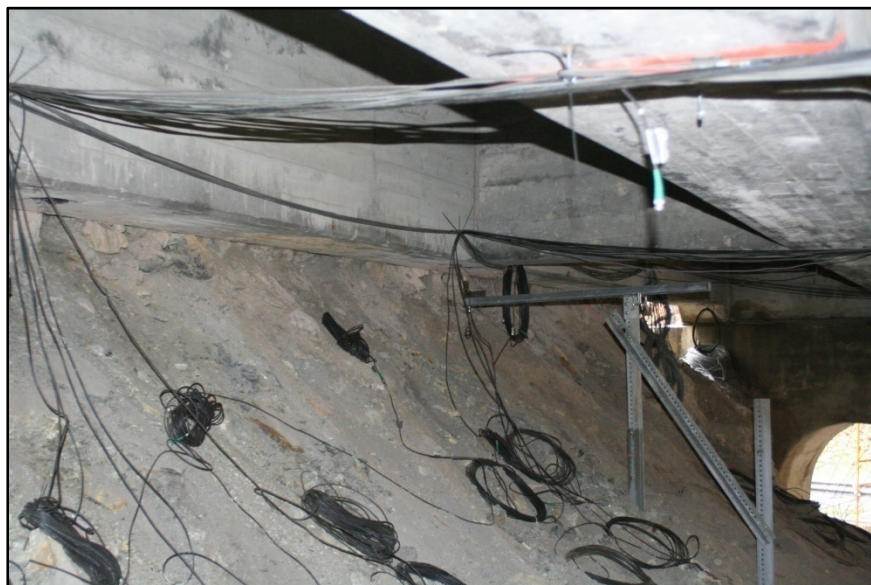


Figure 6-9 - Beam in Contact with the Ground

6.2.2 Michigan Avenue Results

As discussed previously, the responses measured during the Michigan Avenue test were limited to displacements since there was no rebar present in the arch, and it was difficult to locate in the beams. Up until the final load stage, the beams and the arch were responding linearly. The test was stopped early when a substantial change in the stiffness of the structure was noted, resulting in some residual displacement. This can be seen in load versus displacement plot including unloading from the final load stage, shown in Figure 6-10.

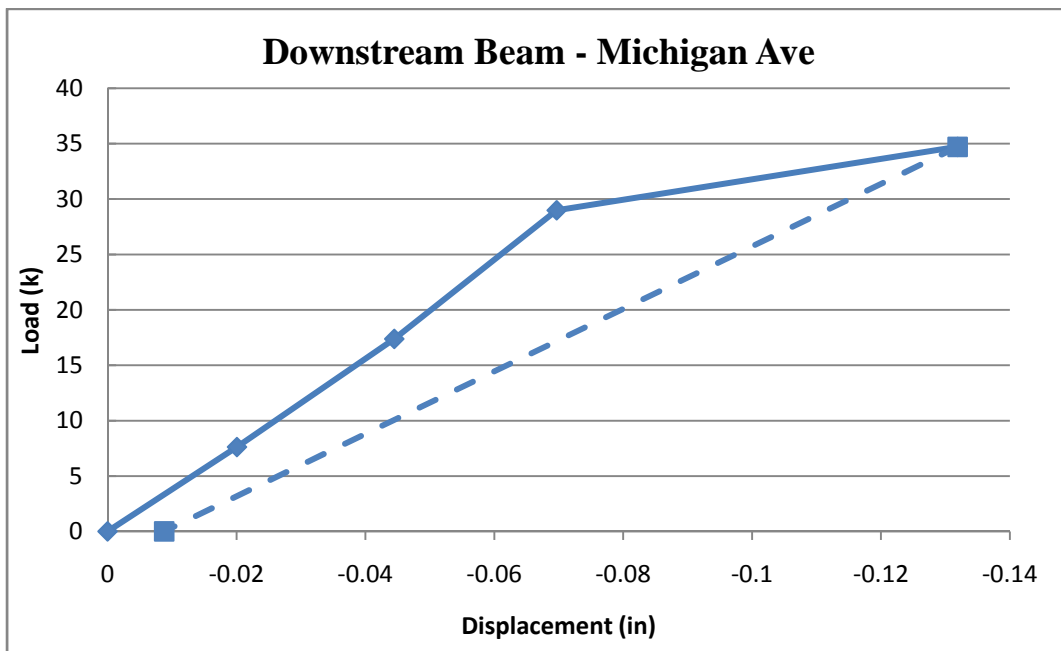


Figure 6-10 - Load versus Displacement of the Downstream Beam

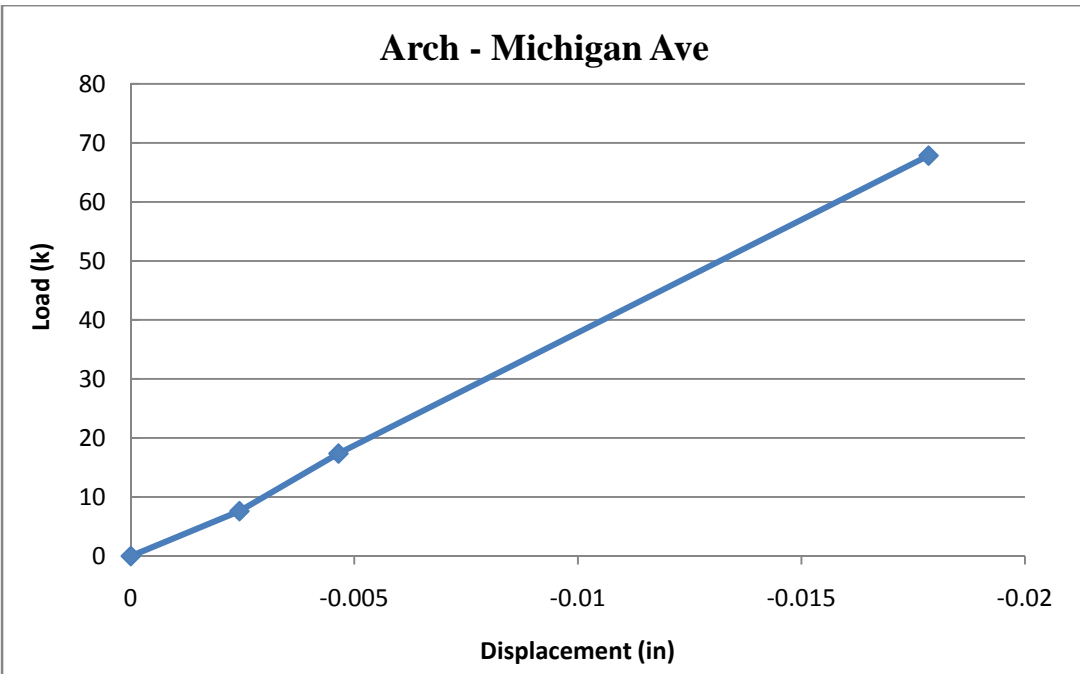


Figure 6-11 - Load versus Displacement of the Downstream Beam

6.3 Proof Level Load Rating

6.3.1 Smithers Bridge Load Rating

Load ratings were calculated for the Smithers Bridge at both inventory and operating level using the NCHRP Manual for Bridge Rating through Load Testing. The rating is based on the 80k non-CRTS state load level truck. At both inventory and operating, the bridge rated greater than 1. The ratings are presented below in Table 6-1.

Table 6-1 - Proof Level Rating Factors - Smithers

	Operating	Inventory
Rating (80 k)	4.0	2.9

6.3.2 Michigan Avenue Bridge Load Rating

Load ratings were calculated for the Smithers Bridge at both inventory and operating level using the NCHRP Manual for Bridge Rating through Load Testing. **The rating is based on the posting of 9 tons.** At both inventory and operating, the bridge rated less than 1. The ratings are presented below in Table 6-2.

Table 6-2 - Proof Level Rating Factors - Michigan Avenue

	Operating	Inventory
Rating (9 tons)	0.94	0.69

7 Experiment and Instrumentation Design – Dynamic Test

7.1 Excitation Methods

7.1.1 Instrumented Sledgehammer

The instrumented sledgehammer is a 25 lb sledgehammer from PCB Piezoelectronics with a load cell embedded in the impact head. The impact head allows for different tips to be affixed to the end to vary the frequency range of the input. The impact tips range from grey (super-soft – low frequency range) to black (hard plastic – high frequency range).

7.1.2 Falling Weight Deflectometer (FWD)

FWD's are used for testing of pavement quality. They are comprised of a drop weight device, an array of velocity sensors called geophones, and a load cell used to measure the impact force. The weight is dropped and the sensors pick up peak velocity and force readings. These readings are correlated through empirical relationships to determine the quality of the pavement and the underlying structure.



Figure 7-1 - Falling Weight Deflectometer

This FWD has been partially modified in an effort to develop a bridge screening tool which can impart and impact to a structure and measure the response time histories. The modifications were tested on the Smithers Bridge.

7.1.3 Drop Hammer Machine

A drop hammer machine was designed and constructed for the purpose of making alterations to the impact method utilized by the FWD without concern of permanent damage. The drop hammer machine is basically a manually operated FWD without any additional sensors or data acquisition. It is comprised of a steel box frame, two aluminum tracks and an impact carriage that is raised up using a hand winch and dropped via quick release, creating an impact on the structure. The drop hammer is shown in Figure 7-2. This was also used to impact the Smithers Bridge.



Figure 7-2 - Drop Hammer Machine

7.2 Instrumentation Selection

7.2.1 Sensor Selection

Two types of accelerometers were available for the dynamic testing of the Smithers Bridge.

These included piezoelectric and capacitive type accelerometers from PCB Piezoelectronics Inc.

The piezoelectric accelerometer, shown in Figure 7-3, was the Model 393C seismic accelerometer which was used on the underside of the bridge. This accelerometer uses the piezoelectric effect of quartz to directly convert acceleration to a low impedance voltage signal.

The voltage signal produced is proportional to the vibratory force experienced by the accelerometer. The low-impedance output signal can be transmitted over very long distances with minimal signal degradation using regular coaxial cable. The stainless steel sensor housing is hermetically sealed and contains the crystals, a seismic mass, and a low noise electronic amplifier. The Model 393C accelerometer is a unidirectional sensor; therefore, it can only measure accelerations in one principal direction. A total of 8 of these accelerometers were used for the dynamic test.

The Model 3701 accelerometer, shown in Figure 7-4, was the capacitive type of accelerometer which was not used for this test. This accelerometer uses an air-damped, opposed-plate capacitor and the sensing element. Once energized, the accelerometer generates a low-impedance voltage output that is directly proportional to acceleration. The low impedance output signal can be transmitted over long distances with minimal signal degradation using ordinary wires. Capacitive accelerometers can measure frequencies all the way to DC (0 Hz). The tolerances of the internal electrical components give this accelerometer a zero-g offset voltage. The voltage offset is generally less than 200 mV and could be nulled by the zero-adjust feature on the capacitive accelerometer signal conditioners. The Model 3701 accelerometer requires a three-conductor

cable, with one conductor to carry the excitation power, one conductor for carrying the measurement signal, and the final conductor serving as a common ground. This particular accelerometer is also a unidirectional sensor.



Figure 7-3 - Piezoelectric Accelerometer



Figure 7-4 - Capacitive Accelerometer

7.2.2 Data Acquisition

The HBM data acquisition system is composed of a chassis and up to sixteen interchangeable cards. For this test, three cards which have eight channels each. The HBM has a 24 bit Analog to

Digital Converter for processing of the analog voltage signal put out by the sensors. Data is synchronously sampled at 52,000 Hz and then decimated down to a maximum of 2,400 Hz.

7.2.3 Layout and Reasoning – Smithers Bridge

As with the static instrumentation, the dynamic layout was heavily focused on the first span, which can be seen in Figure 7-5. An effort was made to have one entire longitudinal grid line instrumented, though the location at F5 was unreachable. Otherwise, every point which had a displacement measurement had an acceleration to provide the opportunity to compare to modal and static flexibility.

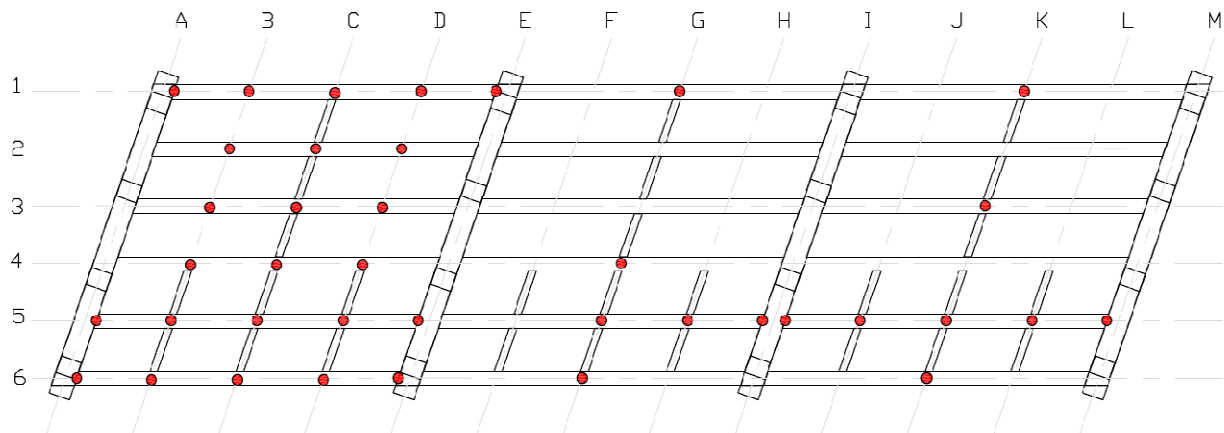


Figure 7-5 - Smithers Bridge Dynamic Instrumentation Layout

7.2.4 Layout and Reasoning –Michigan Avenue Bridge

The Michigan Avenue Bridge was most heavily instrumented along the midline. From prior experience, little response was expected from the arch, and therefore no sensors off of the midline were installed on the arch. The more flexible beams had gages installed at quarter and three-quarter span as well as the midline. The layout can be seen in Figure 7-6.

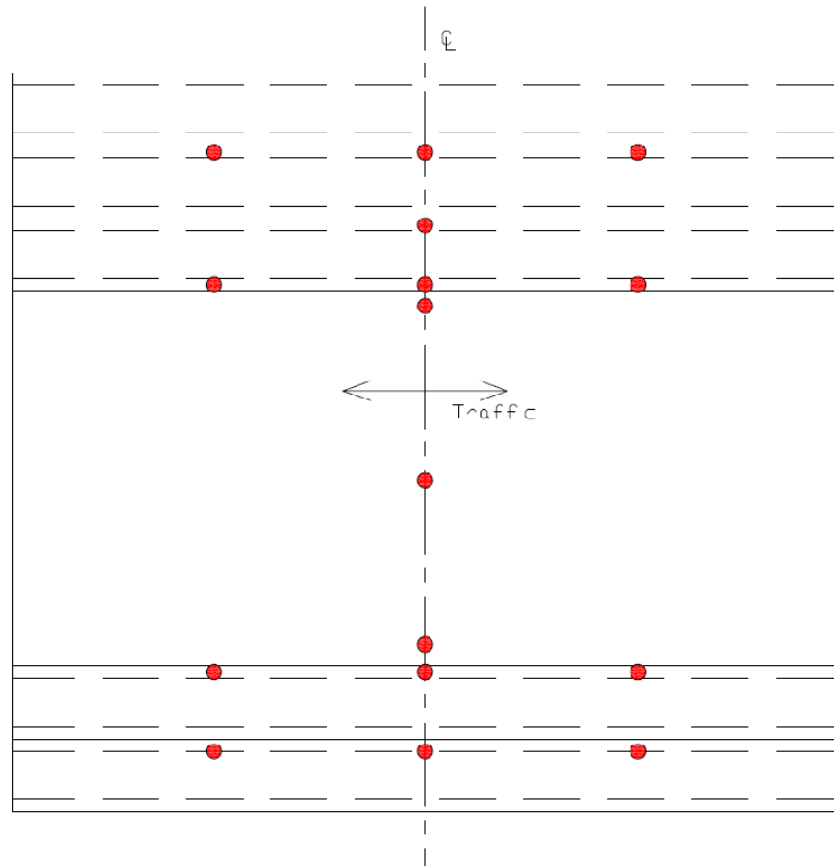


Figure 7-6 - Michigan Ave Bridge Dynamic Instrumentation Layout

8 Dynamic Test Results

8.1 Dynamic Test Summary – Smithers Bridge

The first dynamic test consisted of striking the bridge in several locations with an instrumented sledge hammer shown in Figure 8-1. The second test utilized the FWD as the impact device, shown in Figure 8-3. The third test involved using an instrumented drop weight device to impact the deck of the structure. The drop weight device is shown in Figure 8-2.

8.1.1.1 Impact on topside

The instrumented sledgehammer was used to impact the topside of the bridge at 37 different locations. The grid pattern of impacts matches the accelerometer layout which is discussed in section 7.2.3.



Figure 8-1 - Impact on the Top Side of the Bridge

Typically, impacts on the topside of the structure with the instrumented sledgehammer were approximately 5000 lbs.

8.1.2 Drop Hammer Machine

Three locations on the top side of the bridge were impacted with the drop hammer in a diagonal pattern. The three points coincide with the locations at which the sledgehammer tests were conducted. At each test location, a total of three impacts were done. The drop hammer on the bridge can be seen in Figure 8-2.



Figure 8-2 - Drop Hammer Test on the Bridge

8.1.3 Falling Weight Deflectometer

The modified falling weight deflectometer was used to impact the top surface of the bridge at 9 locations, all of which correspond to prior tests. At each point a total of 5 impacts were completed.



Figure 8-3 - FWD Testing on the Bridge

8.1.4 Dynamic Test Results

8.1.4.1 Sledgehammer Results

The MIMO testing configuration was used for testing the Smithers Bridge utilizing all excitation devices. A sample set of FRFs for the Smithers Bridge resulting from the sledgehammer are shown in Figure 8-4. This test resulted in the identification of five poles between 10 and 50 Hz.

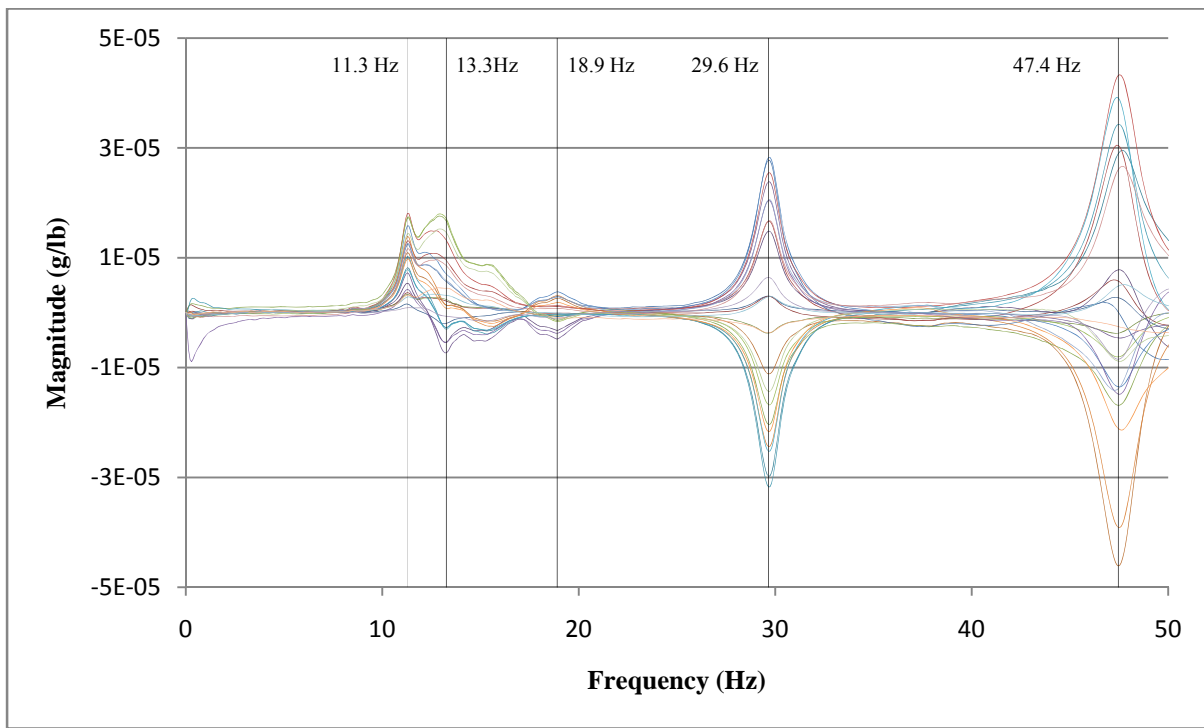
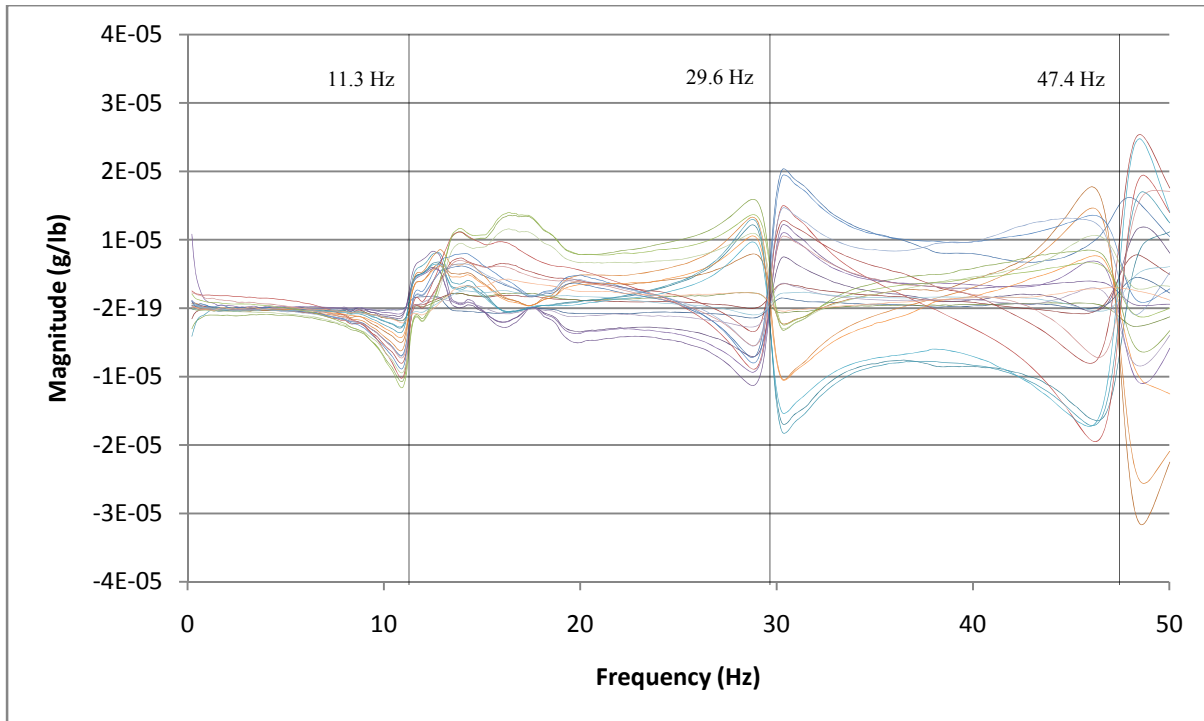


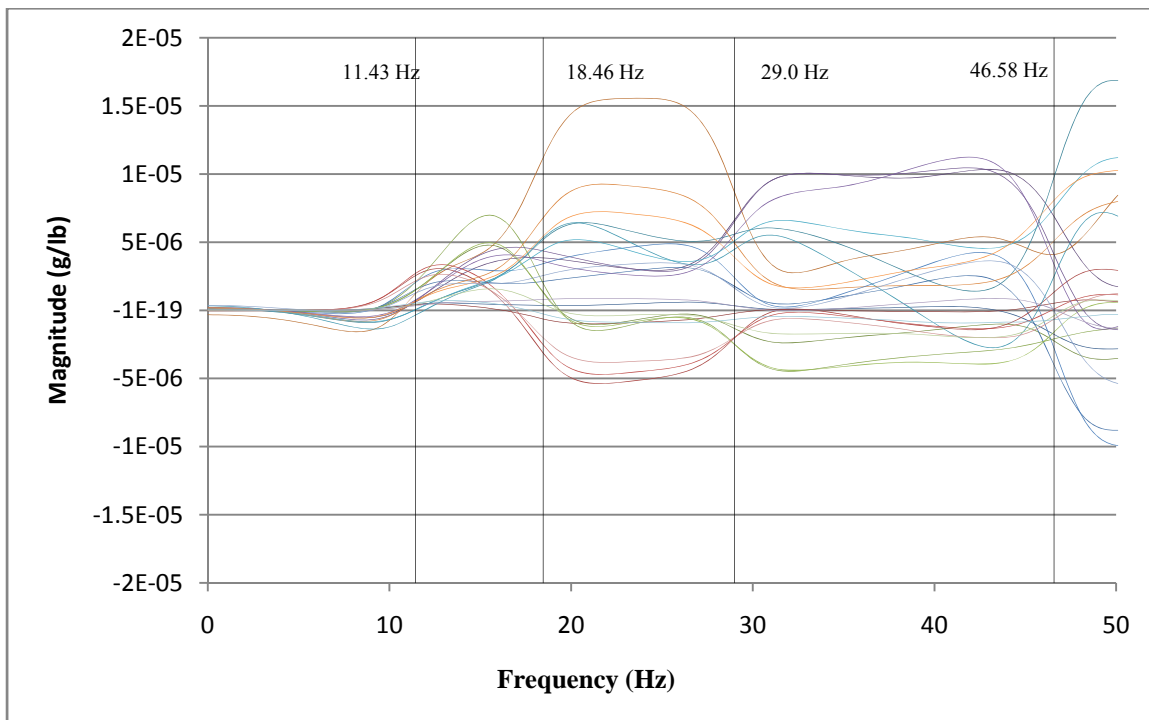
Figure 8-4 (a) Real portion of the FRF derived from MIMO test on deck, (b) Imaginary portion of the FRF derived from MIMO test on deck

8.1.4.2 Drop Hammer Results

A set of FRFs for the Smithers Bridge resulting from the drop hammer are shown in Figure 8-5.

This test using the drop hammer resulted in the identification of four poles between 10 and 50 Hz.

These FRF's result from impact at a single location and provided as an example. Depending on the location of the impact, other frequencies may be detected. Note that the FRF's for the drop hammer tend to be much smoother than the sharp peaks provided by the sledge hammer.



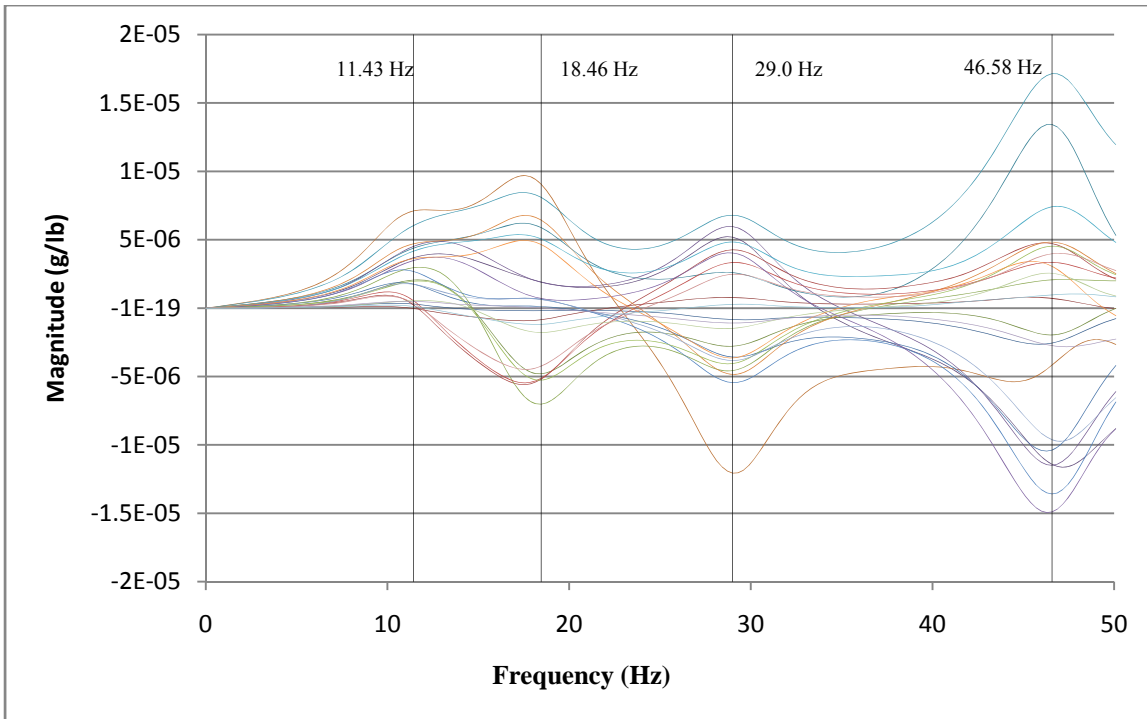


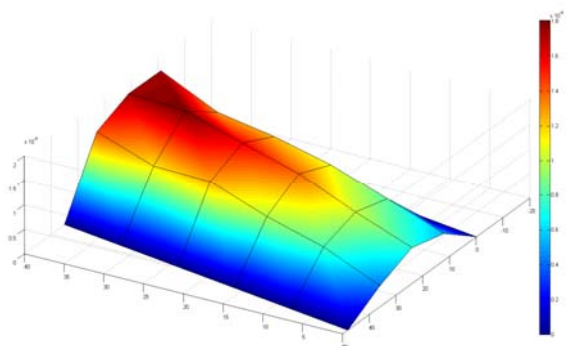
Figure 8-5: (a) Real portion of the FRF derived from MIMO test using the drop hammer, (b) Imaginary portion of the FRF derived from MIMO test using the drop hammer

8.1.4.3 Falling Weight Deflectometer Results

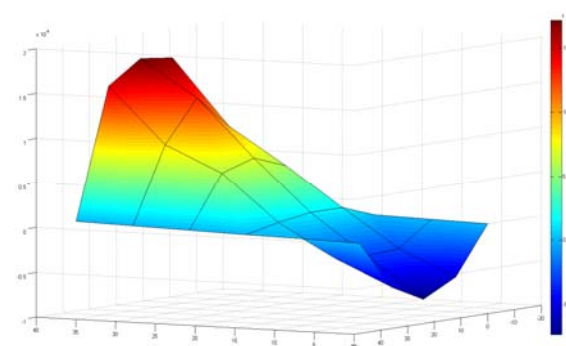
While the Falling Weight Deflectometer was used to impact the structure, there was a problem with the data collection of the force time history from the load cell installed within the FWD. The load cell is generally powered through the van which is used to operate the drop weight mechanism. This is equipped with a data acquisition which only records maximum response, not time histories. For this reason, the load cell signal must be directed to a separate data acquisition and an external DC power supply must be present. The HBM dynamic data acquisition system can power all of the sensors, but is not strong enough to power the load cell in the FWD. Since no external power supply was available, it was impossible to measure the force time history, and therefore impossible to determine the FRF's from the FWD response.

8.1.4.4 Mode Shapes and Frequencies

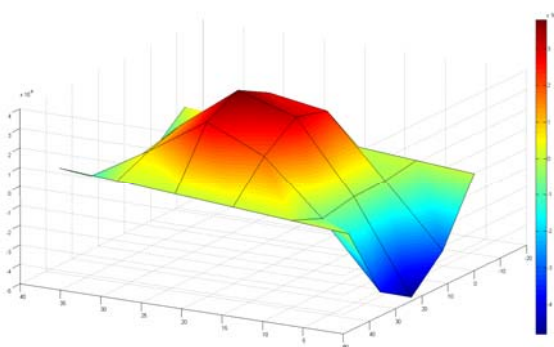
The process of modal analysis described in Section 9.1 and 9.2 was applied to the data from the sledge hammer test. The mode shapes and corresponding natural frequencies of vibration are shown in Figure 8-6. These plots are indicative of the first span and the lines with zero amplitude represent the abutment and pier boundary conditions.



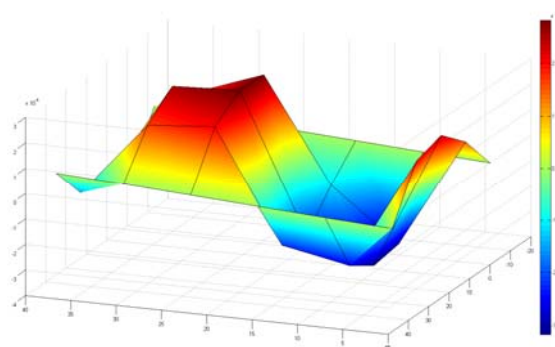
Mode #1 – 11.3 Hz



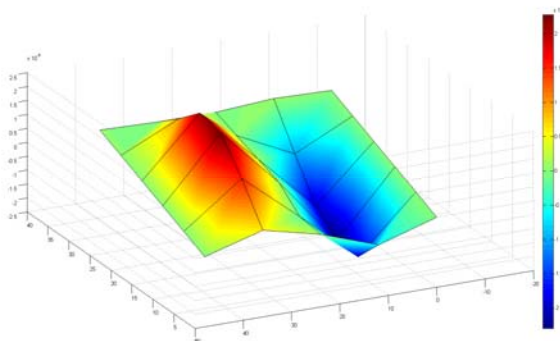
Mode #2 – 13.3 Hz



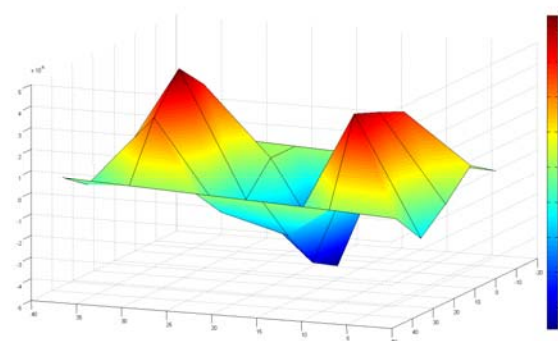
Mode #3 – 18.9 Hz



Mode #4 – 29.7 Hz



Mode #5 – 37.9 Hz



Mode #6 – 47.4 Hz

Figure 8-6 - Mode Shapes from Sledgehammer Test

8.2 Dynamic Test Summary – Michigan Avenue Bridge

Due to the lively nature of the Michigan Avenue Bridge, only a sledgehammer impact test was conducted from the three impact methods. There were 15 impact locations, corresponding to the locations where accelerometers were installed on both the beams and the arch. Additionally, a test using the electromagnetic shaker was conducted. However, based on the definitive results of the static test, the processing of the Michigan Avenue dynamic data has become a strictly academic exercise and will not be presented here.

9 Post-Test Finite Element Correlation

9.1 General Calibration Procedure – Heuristic Method

The traditional method of finite element model calibration is conducted by manually minimizing the error between the experimental results and model output. Based on the initial discrepancies between results and model output, adjustments to the model are made, varying material properties, geometry, boundary conditions or part interaction to attempt to reduce the error. These adjustments are based on knowledge of bridges and construction as well as the in-situ properties of the structure being calibrated. For example, if one abutment of a bridge is in the water, then one potential change would be a softening of the foundation in order to represent a scour condition.

9.2 Smithers Bridge Static Calibration

9.2.1 Updated Parameters

The A priori model provided a very close representation of the measured displacements, meaning that the calibration effort to the global response would be minimal. The main modification was the extent and location of damage, which would affect the section properties input into the model.

9.2.1.1 Extent and Location of Damage

At the site, flexural cracking was observed during loading, especially along the four central beams. Without having the details of the reinforcement and spacing in the beam sections, it is not possible to do an exact cracked section analysis and determine the cracked moment of inertia. Additionally, this analysis would serve only as a lower bound as it does not account for the spacing of the cracks or tension stiffening.

9.2.1.2 Final Model Statistics

The model was heavily discretized to minimize the effect of the skew on the shell elements representing the deck, maximize the ability to vary properties, and make the model as accurate as possible. Table 9-1 shows the model statistics in terms of the number of elements and links.

While this was a large model, the computation time was minimal due to the nature of the model and the applied loading.

Table 9-1 - Model Statistics

<i>Model Statistics</i>
1700 Frame Elements
7000 Shell Elements
1900 Rigid Links

9.2.2 Comparison of Calibrated Model to Experiment

9.2.2.1 Comparison of Displacements of the First Span

The main quantity compared between the model and the experiment was displacements.

Displacements are the most reliable measurement taken in the field, and the easiest to use to calibrate a model. Figure 9-1 through Figure 9-3 shows the comparison of displacements along $\frac{1}{4}$, $\frac{1}{2}$ and $\frac{3}{4}$ lines of the first span, while the load was at midspan. Both the $\frac{1}{2}$ and $\frac{3}{4}$ lines are in excellent agreement with the model, while the $\frac{1}{4}$ line was slightly more flexible. However, this difference was an error of less than 10% and was considered acceptable.

Comparison of Experiment to the Model - First Span

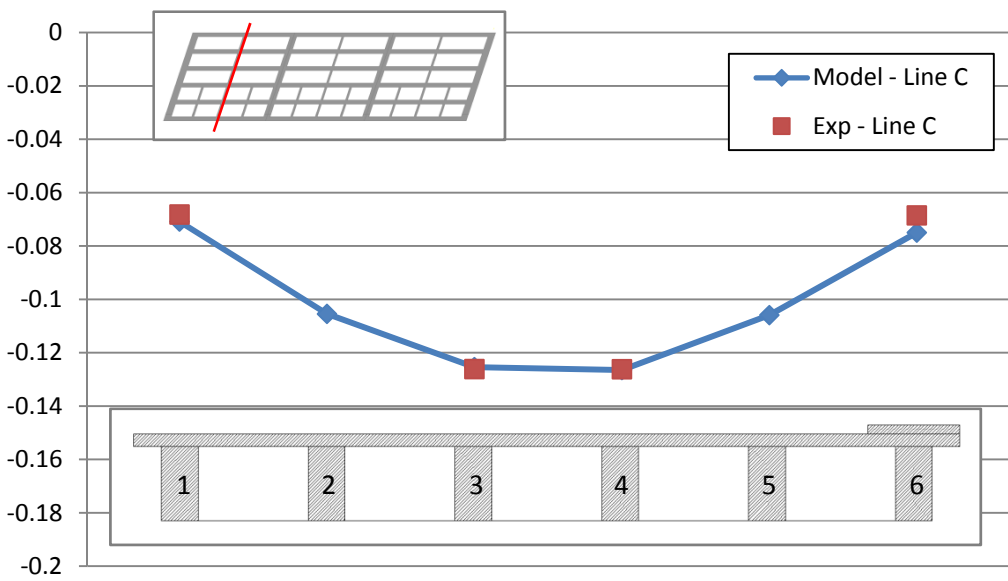


Figure 9-1 - Midspan Displacement Comparison - First Span

Comparison of Experiment to the Model - First Span

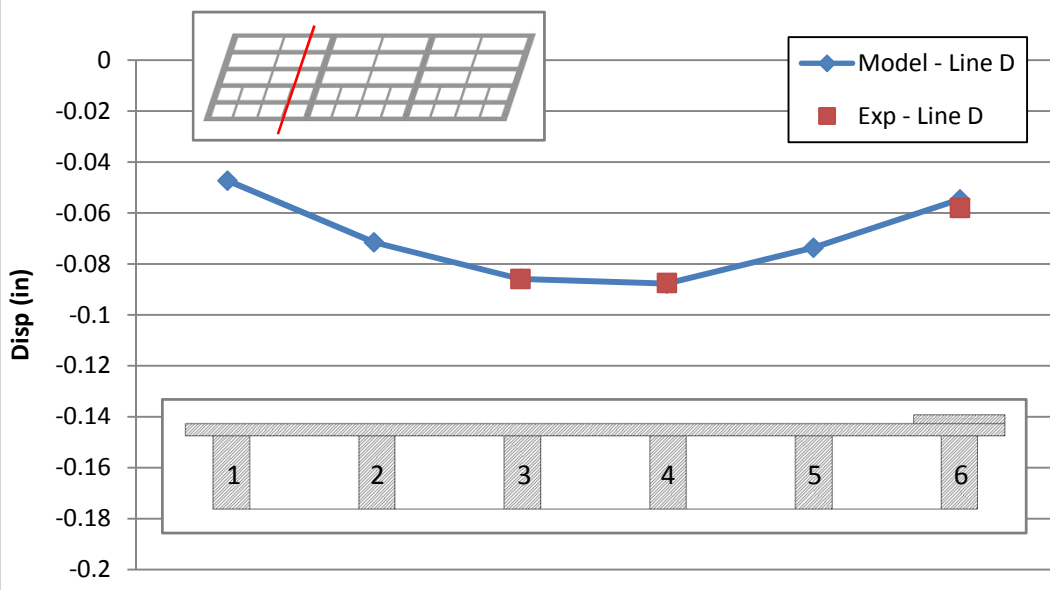


Figure 9-2 – $\frac{3}{4}$ Span Displacement Comparison – First Span

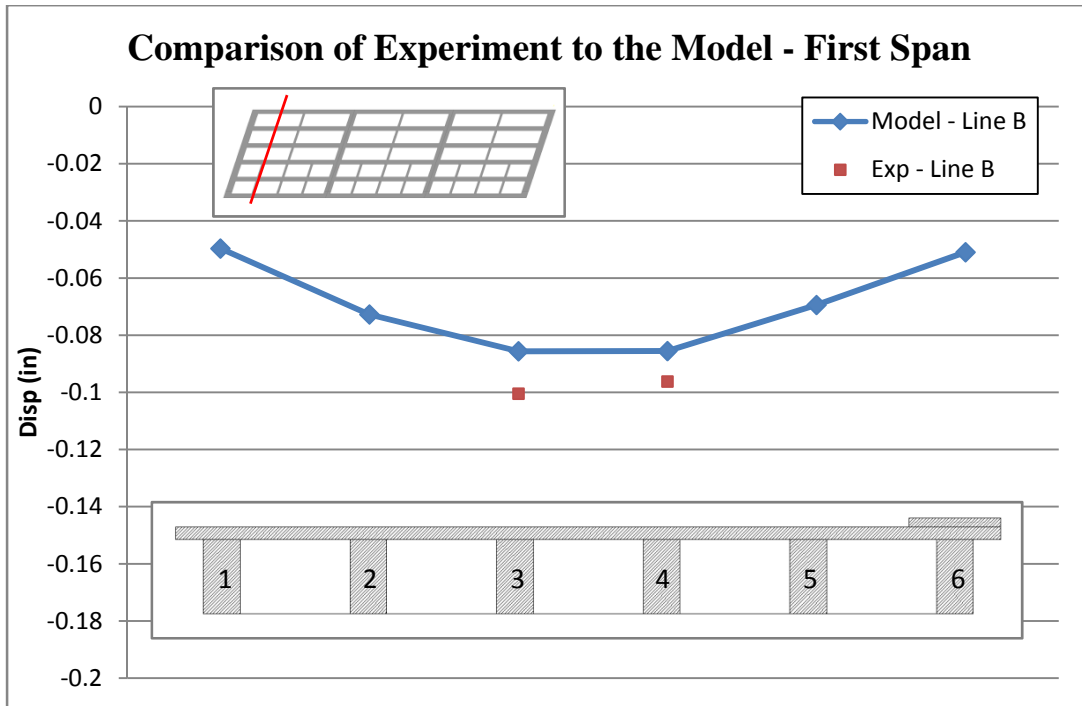


Figure 9-3 - 1/4 Span Displacement Comparison - First Span

9.2.2.2 Comparison of Midline Displacements – Other Spans

The comparisons of displacements from the model to the experiment for the other two spans are shown in Figure 9-4 and Figure 9-5. Both spans show excellent agreement with the model, which indicates that the model is viable for usage in creating load ratings.

Comparison of Experiment to the Model - Second Span

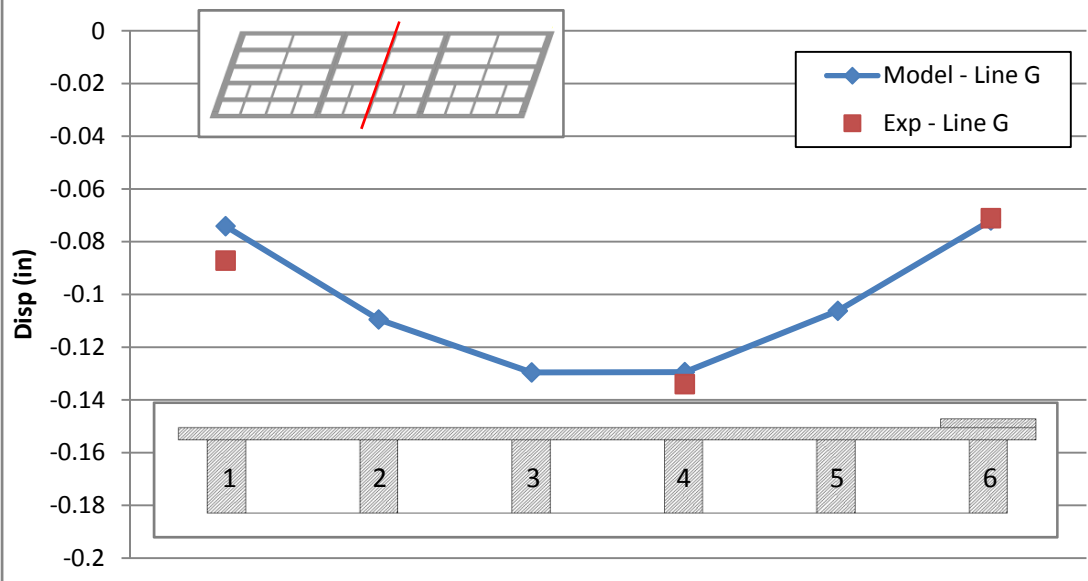


Figure 9-4 - Midline Displacement of Second Span under Load

Comparison of Experiment to the Model - Third Span

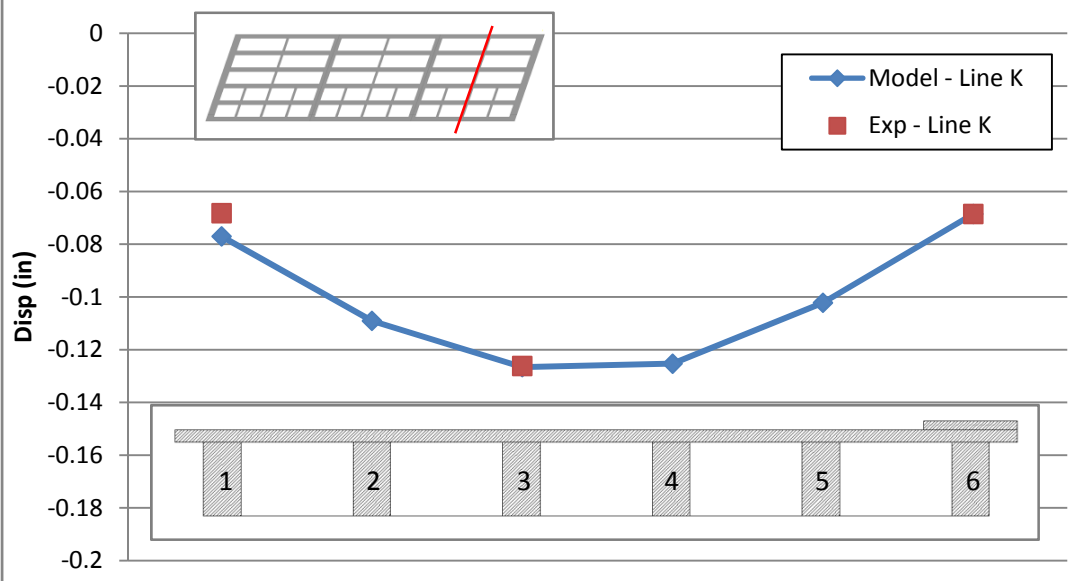


Figure 9-5 - Midline Displacement of Third Span under Load

9.2.3 Calibration to Strain Data

The efforts to calibrate the model to the strain data did not yield acceptable results through application of changes to gross materials properties, as was the case with the displacement data. This indicates that though the strains measured during the load test were a result of the loading on the structure, a disconnect exists between that data and the global response to the structure. This disconnect happens because strain measurements are inherently local, and are susceptible not only to global changes such as boundary conditions, but are also susceptible to localized changes to material or section properties. In other words, a crack in the real structure could be represented as a substantial decrease in stiffness at a localized point, which would correlate directly with the measured strain, but have no impact on the displacements. Taken in this light, the effort to change local properties to match measured strain values becomes trivial. For this reason, the displacement calibration, which is indicative of the global behavior, is used to produce additional load ratings.

9.2.4 Load Rating with Calibrated Model

The calibrated model was used to calculate updated load ratings based on the 40 ton state legal truck for which the bridge is posted. The load rating is for flexure of the beams, and is based on the worst case demand, calculated using a moving load on the calibrated model. The ratings are shown in Table 9-2.

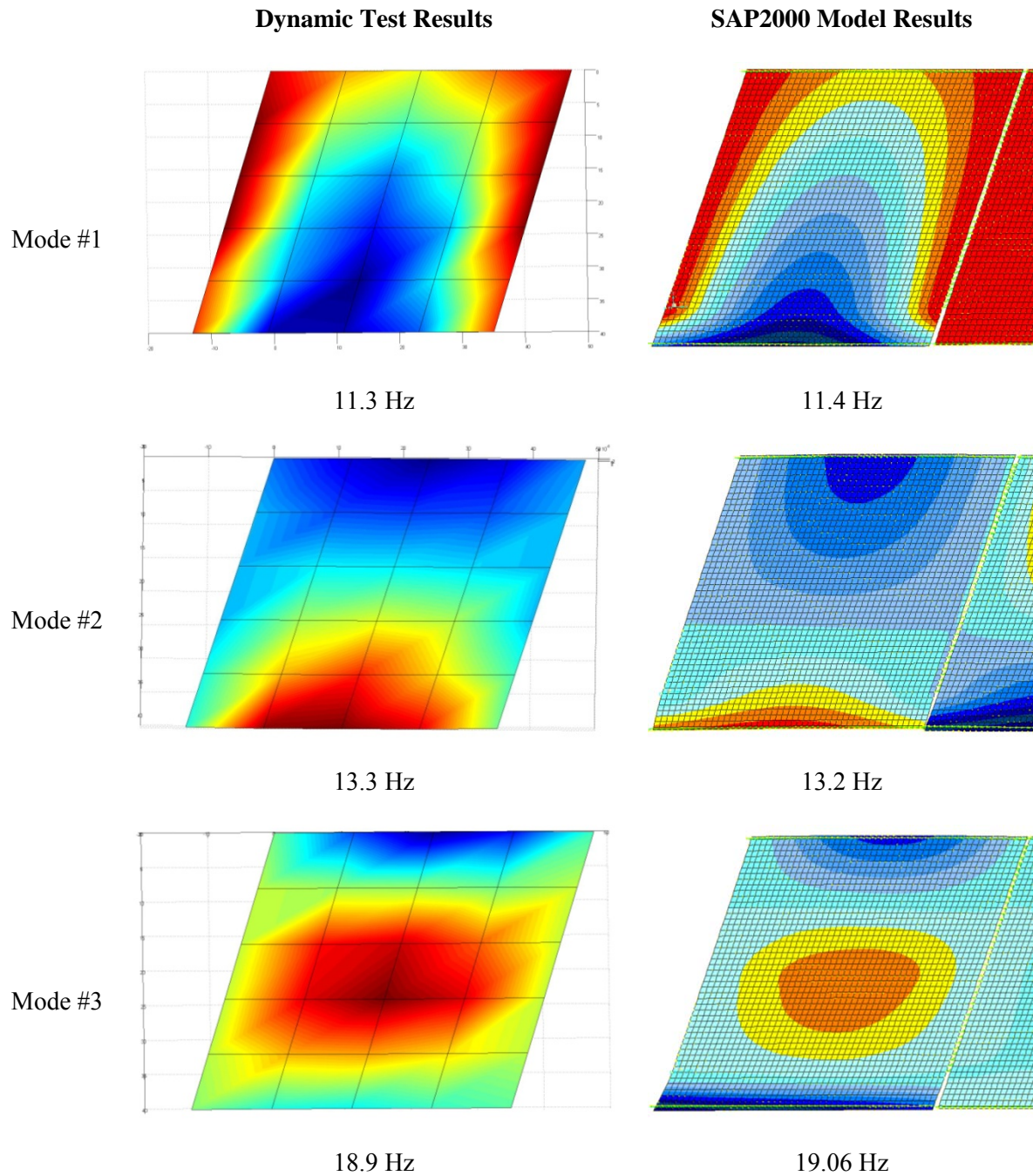
Table 9-2- Load Ratings from Calibrated Model

	<i>Operating</i>	<i>Inventory</i>
Load Rating	3.3	2.6

9.3 Smithers Bridge Dynamic Calibration

After the model was calibrated to the static test results, a comparison of the mode shapes and frequencies from the model was compared to those from the dynamic tests. The model, with only slight adjustments to the mass, compared very well with the dynamic test results. The first three modes in particular were easy to identify in both the model and the dynamic test results and correlated extremely well. These mode shapes are shown in Table 9-3.

Table 9-3 - Mode Shape Comparison



10 Summary, Conclusions and Recommendations

10.1 Summary of Work Completed

The load testing in Smithers, WV consisted of static proof load and impact testing of two structures, a T-beam bridge and a hybrid concrete arch-prestressed beam bridge. Prior to testing, complete field surveys of the bridges and the site were conducted by DI3 personnel. Material testing was carried out by WVDOT, and used in conjunction with an A priori model of the bridge to calculate pre-test load ratings.

Thorough instrumentation plans were designed and installed on both bridges, considering feasibility, expected response levels, and desired responses to best support decision-making. Strains, displacements, rotations and accelerations were measured using a wide array of gages.

The Smithers Bridge was tested to the proof-level load of 600 kips with a maximum strain of 167 $\mu\epsilon$ and a maximum displacement of 0.135 inches. The testing of the Michigan Avenue Bridge was halted prior to reaching the target proof-level load, due to the observation of nonlinear response and permanent deformation. The maximum load achieved during this test was 67 kips, located primarily on the center arch.

The Smithers Bridge test results were used to calibrate a finite element model in SAP2000. The model aligned well with displacement measurements, and was consistent with the observed strains, considering the uncertainty associated with local cracking and tension-stiffening effects. The model also correlated well with the dynamic test results, identifying the first 3 modes very accurately.

10.2 Conclusions

The results of the two load tests, Smithers Bridge and Michigan Avenue Bridge, provided useful insight into the condition, vulnerability and potential life span of both structures.

10.2.1 Smithers Bridge

One purpose of the Smithers Bridge load test was to determine whether the posting at the 40 ton state legal level was required. Based on the load ratings in Table 10-1, it is recommended that the posting be removed.

Table 10-1 - Load Rating Summary

	Proof Level	Calibrated Model
Operating	4	3.3
Inventory	2.9	2.6

However, before this structure can be put into service for an extended period of time, some repairs should be completed. The beam seats, where water draining from the roadway surface has caused spalling and corrosion, should be repaired to a level where there is no exposed rebar. Additionally, the drainage problem should be addressed from the top of the bridge down, to prevent any further damage of this nature. This includes preventing water from infiltrating the top of the bridge at the abutments and piers, and making sure that no water can build up on top of the pier cap between the beams. Any other exposed rebar should be repaired, and the section loss to the pier on upstream side of span #2 should be filled in.

Once these repairs are completed, the WVDOT can consider returning the Smithers Bridge to a standard inspection cycle.

It should be noted that one interesting discovery was that the load ratings indicated by the calibrated model were slightly lower than those of the NCHRP Proof Load Rating procedure. The NCHRP method is considered more conservative than calibration of a finite element model, but in this case the opposite is true. This will be discussed in greater detail in the ensuing research status report.

10.2.2 Michigan Avenue Bridge

The test of the Michigan Avenue Bridge confirmed that the bridge does need to be replaced. The behavior of the beams was such that the posting of 9 tons was unconservative. For this reason, the bridge should be taken to a single lane of traffic until such time as it can be replaced. Limiting all traffic to the arch portion of the structure will mitigate the uncertainty associated with the beams, and ensure all load is taken by the more robust arch.

10.2.3 Research Recommendations and Conclusions

A complete analysis of the Rapid Bridge Screening research, a simplified arch load rating method, and a summary of lessons learned during the load testing process will be presented in a subsequent research summary report.